DEUTSCHES ELEKTRONEN-SYNCHROTRON **DESY**

DESY 89-060
UCLA-89-TEP-22
May 1989

The Physics of the Standard Model

R.D. Peccei

Deutsches Elektronen-Synchrotron DESY

Eigentum der Property of DESY Bibliothek library
Zugang: Accessions: 03. JULI 1989
Leihfrist: Loan period: 7 Tage days

ISSN 0418-9833

NOTKESTRASSE 85 · 2 HAMBURG 52

DESY behält sich alle Rechte für den Fall der Schutzrechtserteilung und für die wirtschaftliche Verwertung der in diesem Bericht enthaltenen Informationen vor.

DESY reserves all rights for commercial use of information included in this report, especially in case of filing application for or grant of patents.

To be sure that your preprints are promptly included in the
HIGH ENERGY PHYSICS INDEX ,
send them to the following address (if possible by air mail) :

DESY
Bibliothek
Notkestrasse 85
2 Hamburg 52
Germany

UCLA 89-TEP 22

ISSN 0418-9833

DESY 89-060
May 1989

The Physics of the Standard Model

R. D. Peccei *†

Deutsches Elektronen-Synchrotron DESY
Hamburg
Fed. Rep. Germany

ABSTRACT

In these lectures, after a brief resumè of the main elements of the standard electroweak model, I discuss the crucial experiments which helped establish the model and its forthcoming tests with high energy e^+e^- colliders.

* Lectures presented at the Winter School of Physics: Cosmology and Elementary Particles, San Juan, Puerto Rico, March 1988. To appear in the Winter School Proceedings.

† Present address: Department of Physics, UCLA, Los Angeles, California, 90024-11547,USA

I. RESUME OF THE STANDARD MODEL

The standard model of electroweak interactions [1] is a gauge theory based on the group $SU(2) \times U(1)$, which suffers spontaneous symmetry breakdown to $U(1)_{em}$. The theory is fully specified by giving the assignment of the fermionic matter under the gauge group and by detailing the agent of the breakdown. I shall summarize below some of its principal features.

I.1 The Fermion-Gauge Sector

The properties of the left $[f_L = \frac{1}{2}(1-\gamma_5)f]$ and right $[f_R = \frac{1}{2}(1+\gamma_5)f]$ helicity components of the first family of quarks and leptons under $SU(2)\times U(1)$ are detailed in Table I.1 below.

Table I.1: Quantum Number Assignments for the First Family

States	$SU(2)$	$U(1)$	$Q = T_3 + Y$
$\binom{\nu_e}{e}_L$	2	$-\frac{1}{2}$	$\binom{0}{-1}$
e_R	1	-1	-1
$\binom{u}{d}_L$	2	$\frac{1}{6}$	$\binom{\frac{2}{3}}{-\frac{1}{3}}$
u_R	1	$\frac{2}{3}$	$\frac{2}{3}$
d_R	1	$-\frac{1}{3}$	$-\frac{1}{3}$

Note that no right handed neutrino fields are included. These fields may exist, but they are total $SU(2) \times U(1)$ singlets. Note also that the $U(1)$ charge is chosen so that the electromagnetic charge for the various states has the usual values. One has that $Q = T_3+Y$, where T_3 is the 3rd component of the $SU(2)$ generator and Y is the value of the $U(1)$ charge. These same assignments apply also to quarks and leptons of subsequent families. For instance, b_L is part of an $SU(2)$ doublet, while b_R is an $SU(2)$ singlet.

Given the above assignments, the interaction of the fermions with gauge fields is fixed. These interactions arise from replacing ordinary derivatives in the fermion kinetic energic by covariant derivatives leading to an interaction Lagrangian [2]

$$\mathcal{L}_{FG} = gW_a^\mu J_{a\mu} + g'Y^\mu J_\mu \qquad (I.1)$$

In the above W_a^μ and Y^μ are, respectively, the $SU(2)$ and the $U(1)$ gauge fields, with g and g' being the associated coupling constants.

The currents $J_{a\mu}$ and J_μ just reflect the $SU(2)$ and $U(1)$ content of the fermion fields in question and one has, for each fermion f,

$$J_{a\mu} = \bar{f}\gamma^\mu t_a f; \quad J_\mu = \bar{f}\gamma^\mu y f \qquad (I.2)$$

where t_a and y are the $SU(2)$ and $U(1)$ generators respectively, and a sum over both helicities is understood *

It is convenient to rewrite (I.1) in terms of gauge fields of definite charge and mass. For the neutral fields, as we shall check shortly, these are linear combinations of W_3^μ and Y^μ, characterized by the mixing angle Θ_W - the Weinberg angle

$$\begin{pmatrix} W_3^\mu \\ Y^\mu \end{pmatrix} = \begin{pmatrix} \cos\Theta_W & \sin\Theta_W \\ -\sin\Theta_W & \cos\Theta_W \end{pmatrix} \begin{pmatrix} Z^\mu \\ A^\mu \end{pmatrix}, \qquad (I.3)$$

while the fields of definite charge are

$$W_\pm^\mu = \frac{1}{\sqrt{2}}(W_1^\mu \mp iW_2^\mu) \qquad (I.4)$$

In view of Eq (I.4), it is useful to introduce charged currents

$$J_\pm^\mu = 2(J_1^\mu \mp iJ_2^\mu) \qquad (I.5)$$

* $t_a = \frac{\tau_a}{2}$ for the $SU(2)$ doublet fields, but $t_a = 0$ for the singlet fields.

In addition, one can replace the $U(1)$ current J^μ by a combination of the electromagnetic current and J_3^μ. Since $Q = T_3 + Y$, one has

$$J^\mu = J_{em}^\mu - J_3^\mu \qquad (I.6)$$

With the above substitutions the interaction Lagrangian of Eq (I.1) becomes

$$\begin{aligned} \mathcal{L}_{FG} = {} & \frac{1}{2\sqrt{2}} g[W_+^\mu J_{-\mu} + W_-^\mu J_{+\mu}] \\ & + [(g\cos\Theta_W + g'\sin\Theta_W)J_3^\mu - g'\sin\Theta_W J_{em}^\mu]Z_\mu \\ & + [g'\cos\Theta_W J_{em}^\mu + (g'\cos\Theta_W - g\sin\Theta_W)J_3^\mu]A_\mu \end{aligned} \qquad (1.7)$$

If one wants to identify A_μ as the photon field, whose coupling is truly to J_{em}^μ with strength e, then one must impose the, so called, unification condition:

$$e = g'\cos\Theta_W = g\sin\Theta_W \qquad (I.8)$$

Using (I.8), the interaction term in (I.7) involving the other neutral field, Z_μ, reduces to

$$\mathcal{L}_{NC} = \frac{e}{2\cos\Theta_W \sin\Theta_W} J_{NC}^\mu Z_\mu \qquad (I.9)$$

with

$$J_{NC}^\mu = 2(J_3^\mu - \sin^2\Theta_W J_{em}^\mu) \qquad (I.10)$$

Thus for each fermion f one has

$$\begin{aligned} J_{NC}^\mu &= 2[\bar{f}\gamma^\mu t_3 f - \sin^2\Theta_W \bar{f}\gamma^\mu Q_f f] \\ &\equiv 2\bar{f}[\gamma^\mu V_f + \gamma^\mu\gamma_5 A_f]f \end{aligned} \qquad (I.11)$$

Using Table I.1 it is easy to see that

$$\begin{aligned} V_f &= \frac{1}{2}(t_3)_{f_L} - Q_f \sin^2\Theta_W \\ A_f &= -\frac{1}{2}(t_3)_{f_L} \end{aligned} \qquad (I.12)$$

For weak processes where the momentum or energy transfer q^2 is much less than the mass squared of the weak bosons, the interaction terms in (I.7) and (I.9) can be replaced by an effective current current Lagrangian.

$$\begin{aligned}\mathcal{L}_{eff}^{weak} &= \frac{i}{2}\int \mathcal{L}_{FG}\ \mathcal{L}_{FG} \\ &\simeq (\frac{e}{2\sqrt{2}\sin^2\Theta_W})^2 \frac{1}{M_W^2} J_+^\mu J_{-\mu} + \frac{1}{2}(\frac{e}{2\sin\Theta_W\cos\Theta_W})^2 J_{NC}^\mu J_{NC\mu}\end{aligned} \tag{I.13}$$

Since the charged current interactions in the limit of $q^2 << M_W^2$ must reproduce the Fermi theory

$$\mathcal{L}_{Fermi} = \frac{G_F}{\sqrt{2}} J_+^\mu J_{-\mu}, \tag{I.14}$$

one identifies

$$\frac{G_F}{\sqrt{2}} = \frac{e^2}{8\sin^2\Theta_W M_W^2} \tag{I.15}$$

which is a formula for the W mass, once $\sin^2\Theta_W$ is determined experimentally.* Using this identification and introducing a parameter

$$\rho = \frac{M_W^2}{\cos^2\Theta_W M_Z^2}, \tag{I.16}$$

one can rewrite the effective weak Lagrangian of the Glashow Salam Weinberg model as

$$\mathcal{L}_{eff}^{weak} = \frac{G_F}{\sqrt{2}}[J_+^\mu J_{-\mu} + \rho J_{NC}^\mu J_{NC\mu}] \tag{I.17}$$

* Using $G_F \simeq 10^{-5} GeV^{-2}$ and $\sin^2\Theta_W \simeq 0.25$ one has $M_W \simeq 80\ GeV$, so that the approximation of $q^2 << M_W^2$ is very reasonable for all present experiments, except those involving direct W - production.

I.2 The Pure Gauge Sector

The interaction of the $SU(2)$ and $U(1)$ gauge fields are also fixed by local gauge invariance. The Lagrangian which contains the kinetic energy term for the gauge fields also contains interaction terms dictated by the symmetry. One has

$$\mathcal{L}_G = -\frac{1}{4}F_a^{\mu\nu}F_{a\mu\nu} - \frac{1}{4}Y^{\mu\nu}Y_{\mu\nu} \tag{I.18}$$

In the above $F_a^{\mu\nu}$ and $Y^{\mu\nu}$ are the $SU(2)$ and $U(1)$ field strengths [2]:

$$\begin{aligned}F_a^{\mu\nu} &= \partial^\mu W_a^\nu - \partial^\nu W_a^\mu + ig\epsilon_{abc}W_b^\mu W_c^\nu \\ Y^{\mu\nu} &= \partial^\mu Y^\nu - \partial^\nu Y^\mu\end{aligned} \tag{I.19}$$

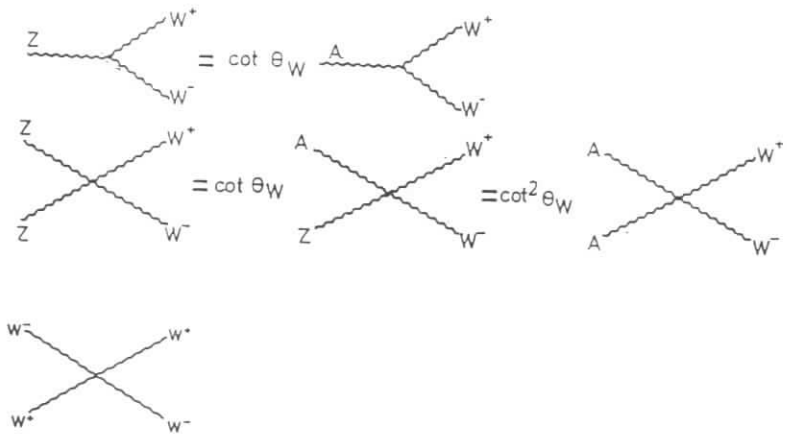

Fig. I.1 Non Vanishing 3-and 4-gauge vertices

The nonlinear terms in the $SU(2)$ field strengths lead directly to a self interaction among the gauge fields in (I.18). The presence of the ϵ_{abc} term implies both 3-gauge vertices

[proportional to ϵ_{abc}] and 4-gauge vertices [proportional to $\epsilon_{abc}\ \epsilon_{dcc}$]. Furthermore, since from Eq (I.3) $W_3^\mu = \cos\Theta_W Z^\mu + \sin\Theta_W A^\mu$, it is easy to see that the only non vanishing vertices among the physical gauge fields are those shown in Fig. I.1

These gauge vertices are important for radiative corrections. However, as we shall indicate in Sec III, the 3-gauge vertices involving ZW^+W^- and γW^+W^- already contribute at the Born level in the process $e^+e^- \to W^+W^-$. So the experimental verification of the expected rate for this process will provide the first direct evidence of the non Abelian nature of the electroweak interactions.

I.3 The Symmetry Breaking Sector.

In the simplest version, of the electroweak model the agent for the breakdown of $SU(2) \times U(1)$ to $U(1)_{em}$ is a complex doublet of scalar fields - the Higgs doublet Φ. This field is assumed to have self interactions, described by a potential $V(\Phi)$, whose non trival minimum occurs for a value of Φ which breaks $SU(2) \times U(1)$. Taking this potential as

$$V(\Phi) = \lambda(\Phi^\dagger\Phi - \frac{v^2}{2})^2 \qquad (I.20)$$

it is clear that Φ has a non vanishing vacuum expectation value equal to $\frac{1}{\sqrt{2}}v$. With the definition of charge adopted, if Φ has $y = -\frac{1}{2}$, then the vacuum expectation value

$$< \Phi >= \frac{1}{\sqrt{2}}\begin{pmatrix} v \\ 0 \end{pmatrix}. \qquad (I.21)$$

breaks $SU(2) \times U(1) \to U(1)_{em}$, since $Q < \Phi >= 0$.

Because Φ has $SU(2) \times U(1)$ quantum numbers, to preserve the local symmetry the derivative terms of Φ, appearing in the kinetic energy terms, must be replaced by covariant derivates [2]:

$$\partial_\mu\Phi \to D_\mu\Phi = [\partial_\mu - ig\frac{\tau_a}{2}W_{a\mu} + ig'\frac{1}{2}Y_\mu]\Phi \qquad (I.22)$$

The Higgs kinetic energy term

$$\mathcal{L}_{HG} = -\frac{1}{2}(D_\mu\Phi)^\dagger(D^\mu\Phi) \qquad (I.23)$$

gives rise to mass terms for three out of the four $SU(2) \times U(1)$ gauge fields, when Φ acquires a non zero vacuum expectation value $< \Phi >$. Furthermore, in this processs of mass generation, also three of the four fields in Φ get transmuted into the longitudinal polarization components of the massive gauge fields and one is left with only one physical scalar Higgs field, H. This field has an analogous role to the vacuum expectation value v in Φ, so that the effective replacement of Φ by

$$\Phi \to \frac{1}{\sqrt{2}}\begin{pmatrix} v + H \\ 0 \end{pmatrix} \qquad (I.24)$$

in (I.23) details both which gauge fields get masses and what are the interactions of the physical Higgs field with these gauge fields. Since $< \Phi >\sim \binom{1}{0}$, only the combination of neutral fields $(g\tau_3 W_3^\mu - g'Y^\mu)_{11}$ gets a mass. Using Eq (I.3) and the unification condition (I.8) one sees that

$$gW_3^\mu - g'Y^\mu = \frac{g}{\cos\Theta_W}Z^\mu, \qquad (I.25)$$

so that indeed the field A^μ - which we identified earlier as the photon field - remains massless in the breakdown. A simple calculation then gives for the Z and $W_\pm$ masses the values:

$$M_W = \frac{1}{2}gv; \quad M_Z = \frac{1}{2}\frac{gv}{\cos\Theta_W} \qquad (I.26)$$

Thus, in the case of doublet Higgs breaking, the ρ parameter, typifying the strength of the neutral current (NC) interactions relative to that of the charged currents (CC), is unity:

$$\rho = \frac{M_W^2}{M_Z^2\cos^2\Theta_W} = 1 \qquad (I.27)$$

Using Eq (I.15) one can use the above results to relate the scale v directly to the Fermi constant. One has

$$v = (\sqrt{2}G_F)^{-\frac{1}{2}} \simeq 250\ GeV \qquad (I.28)$$

From Eq (I.23) and the effective replacement (I.24) one deduces immediately the interactions of the Higgs scalar to the gauge fields. For instance, using Eq (I.26), one finds the following trilinear couplings

$$\mathcal{L}_{HG} = -\frac{e}{\sin 2\Theta_W} M_Z Z^\mu Z_\mu H - \frac{e}{\sin \Theta_W} M_W W_+^\mu W_{-\mu} H \qquad (I.29)$$

Note that the Higgs couplings are proportional to the mass of the excitations it couples to. However, the mass of the Higgs field itself is not fixed directly. Using the substitution (I.24) in the potential (I.20) yields for the Higgs mass the expression

$$M_H^2 = 2\lambda v^2, \qquad (I.30)$$

whose scale is fixed by the Fermi scale v, but whose magnitude is unknown, since the Higgs self coupling λ is not yet determined. Indeed, one has no real idea if the Higgs field H itself exists! Its presence is a straight forward prediction of the simple way in which we assumed $SU(2) \times U(1)$ is broken down. In more elaborate dynamical breakdown mechanisms [3], one can remove this excitation from the spectrum. However, it will always get replaced by some other debris, associated with the symmetry breakdown. An important open question in the standard model is to elucidate the nature of the symmetry breakdown. Naturally, a worthwhile goal is to search for the Higgs boson, as this is the direct manifestation of the simplest way to cause the $SU(2) \times U(1) \to U(1)_{em}$ breakdown.

I.4 Yukawa Interactions and Fermion Masses

The existence of a Higgs doublet Φ, with non zero vacuum expectations value $< \Phi >$, is good for another reason. Through Φ and its presumed interactions with the fermions in the theory, these fermions themselves can get masses. Because of the asymmetric assignment of f_L and f_R in Table I.1 under $SU(2)$, direct fermion mass terms

$$\mathcal{L}_{mass} = -m\bar{f}f = -m(\bar{f}_L f_R + \bar{f}_R f_L) \qquad (I.31)$$

are forbidden in the electroweak theory. However, $SU(2) \times U(1)$ is spontaneously broken to $U(1)_{em}$ and this latter symmetry allows for fermion mass terms. So fermion mass terms can be generated after $SU(2) \times U(1) \to U(1)_{em}$.

Since the Higgs doublet field Φ has $y = -\frac{1}{2}$ and its charge conjugate

$$\tilde{\Phi} = i\tau_2 \Phi^* \qquad (I.32)$$

has $y = +\frac{1}{2}$, one can write $SU(2) \times U(1)$ invariant interactions of these fields with the left and right-handed quarks and leptons. For the first family these, so called, Yukawa interactions read

$$\begin{aligned} \mathcal{L}_{FH} = &- \Gamma^u(\bar{u}\bar{d})_L \Phi u_R + \Gamma^d(\bar{u}\bar{d})_L \tilde{\Phi} d_R \\ &+ \Gamma^e(\bar{\nu}_e \bar{e})_L \tilde{\Phi} e_R + h.c. \end{aligned} \qquad (I.33)$$

Clearly, when Φ gets replaced by (I.24), and $\tilde{\Phi}$ by its analogue

$$\tilde{\Phi} \to -\frac{1}{\sqrt{2}} \begin{pmatrix} 0 \\ v + H \end{pmatrix}, \qquad (I.34)$$

these interactions will give rise to mass terms for the charged fermions

$$m_f = \frac{\Gamma^f}{\sqrt{2}} v \qquad (I.35)$$

and to Higgs fermion interactions. The fermion masses, as was the case already for the Higgs boson, are undetermined, since the Γ^f couplings are unknown. However, all masses are proportional to the $SU(2) \times U(1)$ breaking scale v, as they should. Using (I.35), the Higgs fermion couplings take a very simple form.

$$\mathcal{L}_{FH} = -\frac{m_f}{v} \bar{f} f H \qquad (I.36)$$

which again show the characteristic coupling to mass of the Higgs scalar.

Although it is not particularly germane to these lectures, I should mention briefly the principal modification ensuing by considering more than one family of quarks and leptons. In this case, after $SU(2) \times U(1)$ breakdown, one is left with mass matrices for the quarks

and leptons of the same charge. To go to a physical basis, these mass matrices must be diagonalized. This basis change introduces a mixing matrix in the charged current (CC) interactions, the Cabibbo Kobayashi Maskawa matrix [4]. Thus now for example, for the case of three families, besides a $\bar{u}dW^+$ coupling there is also a $\bar{u}sW^+$ and a $\bar{u}bW^+$ coupling. It is easy to see, however, that both the neutral current (NC) and the Higgs interactions will remain flavor diagonal. So, in particular, the formula (I.36) applies also in the case of many fermion generations.

II. EXPERIMENTS WHICH ESTABLISHED THE ELECTROWEAK THEORY

The Glashow Salam Weinberg [1] $SU(2) \times U(1)$ model of the electoweak interactions was established as the standard model only after extensive experimental confirmation in the last 15 years. In this section, I would like to discuss three types of experiments which, in my opinion, had a particularly strong role in singling out the $SU(2) \times U(1)$ model as the standard model of the electroweak interactions. These include:

i) Neutrino neutral current experiments

ii) Interference experiments in deep inelastic scattering

iii) Direct production of Z and W bosons at the CERN – and now at the FNAL – collider

II.1 Neutrino Neutral Current Experiments

I want to consider here two kinds of experiments: elastic neutrino scattering off electrons $[\nu_\mu e \to \nu_\mu e]$ and deep inelastic neutral current neutrino scattering in nuclei $[\nu_\mu N \to \nu_\mu X]$. The former experiments are very clear theoretically but, unfortunately, suffer from a small rate. The latter experiments are less theoretically pristine, but have much larger rates. Basically

$$\frac{\sigma_{\nu_\mu N}}{\sigma_{\nu_\mu e}} \sim \frac{M_N}{m_e} \qquad (II.1)$$

For both processes, at the fundamental level, one needs to compute the cross section for neutrino-fermion NC scattering, with the fermion being, respectively, an electron or one of the quarks inside the nucleons. In the Fermi approximation (i.e., for $q^2 << M^2_Z$) the effective Lagragian for these reactions is given by Eq (I.17). One has

$$\begin{aligned}\mathcal{L}^{eff}_{\nu_\mu f} &= \sqrt{2}G_F\rho(J^\alpha_{NC})_{\nu_\mu}(J_{NC\alpha})_f \\ &= \sqrt{2}G_F\rho[\bar{\nu}_\mu\gamma^\alpha(1-\gamma_5)\nu_\mu][\bar{f}(\gamma_\alpha V_f + \gamma_\alpha\gamma_5 A_f)f]\end{aligned} \qquad (II.2)$$

In what follows, it is somewhat more convenient to rewrite the above in terms of helicity projections of the fermion fields:

$$\gamma_\alpha V_f + \gamma_\alpha\gamma_5 A_f = \gamma_\alpha\frac{(1-\gamma_5)}{2}Q^L_f + \gamma_\alpha\frac{(1+\gamma_5)}{2}Q^R_f \qquad (II.3)$$

with

$$\begin{aligned}Q^L_f &= V_f - A_f = (t_3)_{fL} - Q_f\sin^2\Theta_W \\ Q^R_f &= V_f + A_f = -Q_f\sin^2\Theta_W\end{aligned} \qquad (II.4)$$

where, in the second line, I have made use of Eq (I.12).

Although it is straight forward to compute the scattering cross section for the process $\nu_\mu f \to \nu_\mu f$ or $\bar{\nu}_\mu f \to \bar{\nu}_\mu f$ using the interaction Lagrangian (II.2), it is possible to give a heuristic derivation of the resulting answer which bypasses this calculation altogether [5]. Consider the first of these processes in the CM frame, letting p and p' stand for the 4-momenta of the fermions and ℓ and ℓ' for the 4-momenta of the neutrinos. The CM scattering angle θ^*, in the limit in which one neglects the fermion masses, is trivially related to the kinematic invariant $y = \frac{p\cdot p'}{p\cdot\ell}$:

$$\cos\theta^* = 1 - 2y \qquad (II.5)$$

The interactions in $\mathcal{L}^{eff}_{\nu_\mu f}$ are helicity conserving at each vertex. This means that the helicity of the scattered fermion is the same as that of the incident fermion. So, since neutrinos are always left handed, one needs to consider only two cases: neutrino scattering off left handed fermions (σ_{LL}) and neutrino scattering off right handed fermions (σ_{LR}). These processes are shown schematically in Fig. II.1.

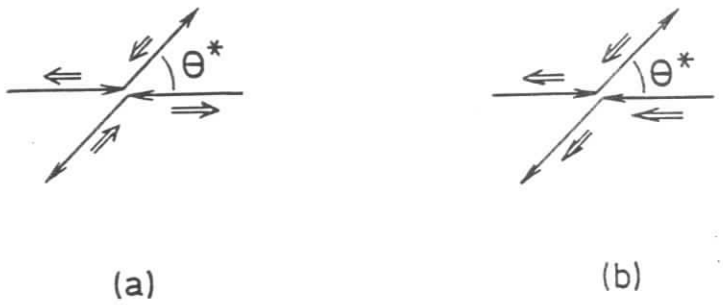

Fig. II.1: Configurations for a) σ_{LL}; b) σ_{LR}

It is immediate from this figure that for the LL process the initial state has $J = 0$. One, therefore, expects an isotropic angular distribution

$$\left(\frac{d\sigma}{d\cos\theta^*}\right)_{LL} \sim 1 \qquad (II.6)$$

On the other hand, for the LR process the backward final configuration has an angular momentum jump of $\Delta J = 2$ and is clearly forbidden. Thus one is led to a distribution

$$\left(\frac{d\sigma}{d\cos\theta^*}\right)_{LR} \sim \left(\frac{1+\cos\theta^*}{2}\right)^2 \qquad (II.7)$$

For antiparticles helicities are interchanged ($L \leftrightarrow R$)*. However, the dynamical considerations for the scattering processes are similar and one deduces analogous results. In view of the kinematical relation (II.5), one arrives at the useful results:

$$\begin{aligned}\left(\frac{d\sigma}{dy}\right)_{LL} &= \left(\frac{d\sigma}{dy}\right)_{RR} \sim 1 \\ \left(\frac{d\sigma}{dy}\right)_{LR} &= \left(\frac{d\sigma}{dy}\right)_{RL} \sim (1-y)^2\end{aligned} \qquad (II.8)$$

* i.e., antineutrinos are always right handed.

The above results makes the structure of the answer for the differential cross section for $\nu_\mu e$ and $\bar{\nu}_\mu e$ scattering, obtained by a direct calculation, very clear. One finds

$$\left(\frac{d\sigma}{dy}\right)^{\nu_\mu e} = \frac{2G_F^2 m_e E_\nu \rho^2}{\pi}\left\{(Q_e^L)^2 + (Q_e^R)^2(1-y)^2\right\} \qquad (II.9a)$$

$$\left(\frac{d\sigma}{dy}\right)^{\bar{\nu}_\mu e} = \frac{2G_F^2 m_e E_\nu \rho^2}{\pi}\left\{(Q_e^R)^2 + (Q_e^L)^2(1-y)^2\right\} \qquad (II.9b)$$

which just reflect the scattering of neutrinos (or antineutrinos) off left or right polarized electrons, with the characteristic y-dependences given in (II.8). Note that in the laboratory frame $y = \frac{E'_e}{E_\nu}$. That is, y is the ratio of the energy carried away by the scattered electron to that of the incident neutrino.

The cross section ratio of $\nu_\mu e$ scattering to $\bar{\nu}_\mu e$ scattering is independent of ρ and is purely a function of $\sin^2\Theta_W$. Integrating Eqs (II-9) one finds

$$R = \frac{\sigma(\nu_\mu e \to \nu_\mu e)}{\sigma(\bar{\nu}_\mu e \to \bar{\nu}_\mu e)} = \frac{3(Q_e^L)^2 + (Q_e^R)^2}{3(Q_e^R)^2 + (Q_e^L)^2} = \frac{3 - 12\sin^2\Theta_W + 16\sin^4\Theta_W}{1 - 4\sin^2\Theta_W + 16\sin^4\Theta_W} \qquad (II.10)$$

Hence, the measurement of this ratio experimentally affords a clean way to extract a value for this fundamental parameter. Unfortunately, neutrino-electron scattering experiments are statistically limited, because of the very small cross sections involved. Indeed, the present day "high statistics" experiments at CERN and Brookhaven have only of the order of 100 events! Nevertheless, from a measurement of R these experiments arrive at the following values for $\sin^2\Theta_W$:

$$\sin^2\Theta_W = \begin{cases} 0.215 \pm 0.032 \pm 0.012 & \text{CHARM [6].} \\ 0.209 \pm 0.029 \pm 0.013 & \text{E734 [7].} \end{cases} \qquad (II.11)$$

In the above, the first error is statistical and the second is systematic. No electroweak radiative corrections are included in extracting these numbers. However, the errors are large enough that it is not worth worrying about this point here.

From the actual measured values of the neutrino and antineutrino cross sections, using the above values of $\sin^2\Theta_W$, one can then determine the ρ parameter. I quote below the result

of the CHARM collaboration [6] for the actual cross sections.

$$\frac{\sigma(\nu_\mu e \to \nu_\mu e)}{E_\nu} = (1.9 \pm 0.4 \pm 0.4) \times 10^{-42} \frac{\text{cm}^2}{\text{GeV}}$$
$$\frac{\sigma(\bar{\nu}_\mu e \to \bar{\nu}_\mu e)}{E_\nu} = (1.5 \pm 0.3 \pm 0.4) \times 10^{-42} \frac{\text{cm}^2}{\text{GeV}} \qquad (II.12)$$

which leads to

$$\rho = 1.09 \pm 0.09 \pm 0.11 \qquad (II.13)$$

Clearly, this value is perfectly consistent with doublet Higgs breaking, where $\rho = 1$.

More accurate values for $\sin^2\Theta_W$ and ρ come from deep inelastic scattering experiments. In the parton model [8] the process $\nu_\mu N \to \nu_\mu X$ proceeds by the scattering of the neutrinos off one of the virtual particles (quarks or antiquarks) in the nucleons making up the nucleus. The relevant kinematics of the neutrino nucleon scattering process is shown in Fig. II.2.

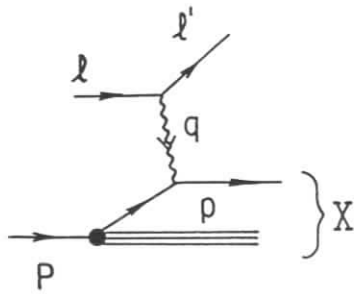

Fig. II.2 Kinematics of neutrino nucleon deep inelastic scattering.

As usual, one defines the kinematical variables

$$x = \frac{-q^2}{2P \cdot q} \quad ; \quad y = \frac{P \cdot q}{P \cdot \ell} \qquad (II.14)$$

If the partons carry a fraction ξ of the nucleon momentum, so that $p^\mu = \xi P^\mu$, then the corresponding variables at the partons level are

$$x_p = \frac{-q^2}{2p \cdot q} = \frac{x}{\xi} \quad ; \quad y_p = \frac{p \cdot q}{p \cdot \ell} = \frac{p \cdot p'}{p \cdot \ell} = y \qquad (II.15)$$

By assumption, in the parton model, the scattering off the various partons in the nucleon is incoherent [8]. Thus, the deep inelastic scattering cross section in the model is given by

$$\frac{d\sigma}{dxdy} = \sum_{\text{parton}} \int_x^1 \frac{d\xi}{\xi} f_{\text{parton}}(\xi; q^2) \frac{d\sigma_{\text{parton}}}{dx_p dy} \qquad (II.16)$$

In the above $f_{\text{parton}}(\xi; q^2)$ is the probability of having a parton with a fraction of momentum ξ in the proton. The q^2-dependence of this probability is a QCD effect [9]. The parton scattering cross section, in lowest order of QCD, is a simple two body scattering process. Hence the parton's fractional ratio x_p is fixed. It is not difficult to convince oneself that $x_p = 1$, so that

$$\frac{d\sigma_{parton}}{dx_p dy} \sim \delta(1 - x_p) \qquad (II.17)$$

The cross sections for deep inelastic neutrino scattering in the parton model are identical to those we detailed earlier for neutrino-electron scattering, except that in this case the targets are quarks and antiquarks with some intrinsic probability distributions $f_q(x; q^2)$. A straightforward calculation, using Eq (II.16), yields the expressions:

$$\left(\frac{d\sigma}{dxdy}\right)^{\nu_\mu}_{NC} = \frac{2G_F^2 M E_\nu \rho^2}{\pi} \left\{ \sum_i x f_{q_i}(x; q^2) \left[(Q^L_{q_i})^2 + (1-y)^2 (Q^R_{q_i})^2 \right] + \sum_i x f_{\bar{q}_i}(x; q^2) \left[(Q^R_{q_i})^2 + (1-y)^2 (Q^L_{q_i})^2 \right] \right\} \qquad (II.18a)$$

$$\left(\frac{d\sigma}{dxdy}\right)^{\bar{\nu}_\mu}_{NC} = \frac{2G_F^2 M E_\nu \rho^2}{\pi} \left\{ \sum_i x f_{q_i}(x; q^2) \left[(Q^R_{q_i})^2 + (1-y)^2 (Q^L_{q_i})^2 \right] + \sum_i x f_{\bar{q}_i}(x; q^2) \left[(Q^L_{q_i})^2 + (1-y)^2 (Q^R_{q_i})^2 \right] \right\} \qquad (II.18b)$$

Note the similarity of these expressions to those in Eq (II.9). The principal difference really is that these cross sections are much larger, since m_e is replaced by the nucleon mass M *. Also here, when one scatters off antiquarks, there is an interchange between the y-dependence of Q^R and Q^L, just as there is this interchange as one passes from neutrino to antineutrino cross sections. That is, one has,

$$\begin{aligned} \nu_\mu &\leftrightarrow \bar{\nu}_\mu \quad : \quad L \leftrightarrow R \\ f_{q_i} &\leftrightarrow f_{\bar{q}_i} \quad : \quad L \leftrightarrow R \end{aligned} \tag{II.19}$$

It is useful to discuss the neutrino neutral current cross sections, given in Eqs (II.18), in the approximation in which the only quarks (and antiquarks) in a nucleon are those in the first family. This, as it turns out, is a pretty good approximation [10] and can always be corrected for in real life. Furthermore, for simplicity, we shall also assume that the nuclear targets used experimentally are isoscalar targets. This again is a good first approximation and small deviations from isoscalarity can also be corrected for. By isospin symmetry, the distribution of $u(d)$ quarks in a proton is the same as that for $d(u)$ quarks in a neutron. If we call the u and d quark distributions in a proton $u(x,q^2)$ and $d(x,q^2)$, respectively, then for an isoscolar target $[N = \frac{1}{2}(n+p)]$ one has, for example,

$$\sum_i x f_{q_i}^N(x;q^2)(Q_{q_i}^L)^2 = \frac{1}{2}x\Big[u(x;q^2)+d(x;q^2)\Big]\Big[(Q_u^L)^2+(Q_d^L)^2\Big] \tag{II.20}$$

with similar expressions for the other distributions entering in Eqs (II.18). Using that

$$\begin{aligned} Q_u^L &= \frac{1}{2} - \frac{2}{3}\sin^2\Theta_W \;;\; Q_u^R = -\frac{2}{3}\sin^2\Theta_W \\ Q_d^L &= -\frac{1}{2} + \frac{1}{3}\sin^2\Theta_W \;;\; Q_d^R = \frac{1}{3}\sin^2\Theta_W \end{aligned} \tag{II.21}$$

a simple calculation yields the formulas

$$\begin{aligned} \Big(\frac{d\sigma}{dxdy}\Big)_{NC}^{\nu_\mu N} = \frac{G_F^2 M E_\nu \rho^2}{\pi}\Bigg\{ & x\Big[u(x;q^2)+d(x;q^2)\Big]\big(A(\Theta_W)+(1-y)^2 B(\Theta_W)\big) \\ & + x\Big[\bar{u}(x;q^2)+\bar{d}(x;q^2)\Big]\big(B(\Theta_W)+(1-y)^2 A(\Theta_W)\big)\Bigg\} \end{aligned} \tag{II.22a}$$

* Note that the weights $\sum_i x f_{q_i}(x;q^2)$ and $\sum_i x f_{\bar{q}_i}(x;q^2)$ entering in Eqs (II.18) have precisely the right normalization. Conservation of momentum leads to the sum rule $\sum_i \int_0^1 dx x f_i(x;q^2) = 1$, so that if there were only one kind of parton, as in $\nu_\mu e$ scattering, then $xf(x) \to 1$.

$$\begin{aligned} \Big(\frac{d\sigma}{dxdy}\Big)_{NC}^{\bar{\nu}_\mu N} = \frac{G_F^2 M E_\nu \rho^2}{\pi}\Bigg\{ & x\Big[u(x;q^2)+d(x;q^2)\Big]\big(B(\Theta_W)+(1-y)^2 A(\Theta_W)\big) \\ & + x\Big[\bar{u}(x;q^2)+\bar{d}(x;q^2)\Big]\big(A(\Theta_W)+(1-y)^2 B(\Theta_W)\big)\Bigg\} \end{aligned} \tag{II.22b}$$

In the above $A(\Theta_W)$ and $B(\Theta_W)$ are given by

$$\begin{aligned} A(\Theta_W) &= \frac{1}{2} - \sin^2\Theta_W + \frac{5}{9}\sin^4\Theta_W \\ B(\Theta_W) &= \frac{5}{9}\sin^4\Theta_W \end{aligned} \tag{II.23}$$

To compare the above (approximate) formulas with experiment, to extract a value of $\sin^2\Theta_W$ and ρ, one needs some information on the parton distribution functions. This can be obviated by using charged current results. With the same approximations, the CC cross sections read

$$\begin{aligned} \Big(\frac{d\sigma}{dxdy}\Big)_{CC}^{\nu_\mu N} = \frac{G_F^2 M E_\nu}{\pi}\Bigg\{ & \Big[x\Big(u(x;q^2)+d(x;q^2)\Big)\Big] \\ & + (1-y)^2\Big[x\Big(\bar{u}(x;q^2)+\bar{d}(x;q^2)\Big)\Big]\Bigg\} \end{aligned} \tag{II.24a}$$

$$\begin{aligned} \Big(\frac{d\sigma}{dxdy}\Big)_{CC}^{\bar{\nu}_\mu N} = \frac{G_F^2 M E_\nu}{\pi}\Bigg\{ & \Big[x\Big(u(x;q^2)+d(x;q^2)\Big)\Big](1-y)^2 \\ & + \Big[x\Big(\bar{u}(x;q^2)+\bar{d}(x;q^2)\Big)\Big]\Bigg\} \end{aligned} \tag{II.24b}$$

Using Eqs (II.24) one can rewrite the NC cross sections as

$$\Big(\frac{d\sigma}{dxdy}\Big)_{NC}^{\nu_\mu N} = \rho^2\Big\{A(\Theta_W)\Big(\frac{d\sigma}{dxdy}\Big)_{CC}^{\nu_\mu N} + B(\Theta_W)\Big(\frac{d\sigma}{dxdy}\Big)_{CC}^{\bar{\nu}_\mu N}\Big\} \tag{II.25a}$$

$$\Big(\frac{d\sigma}{dxdy}\Big)_{CC}^{\bar{\nu}_\mu N} = \rho^2\Big\{B(\Theta_W)\Big(\frac{d\sigma}{dxdy}\Big)_{CC}^{\nu_\mu N} + A(\Theta_W)\Big(\frac{d\sigma}{dxdy}\Big)_{CC}^{\bar{\nu}_\mu N}\Big\} \tag{II.25b}$$

These expressions are known as the Llewellyn Smith relations [10] and, apart from $A(\Theta_W)$ and $B(\Theta_W)$, only involve measureable quantities.

What is actually compared with experiment are the ratios of NC to CC cross sections. If

one defines

$$R_\nu = \frac{\int dxdy(\frac{d\sigma}{dxdy})^{\nu_\mu N}_{NC}}{\int dxdy(\frac{d\sigma}{dxdy})^{\nu_\mu N}_{CC}} \qquad (II.26a)$$

$$R_{\bar{\nu}} = \frac{\int dxdy(\frac{d\sigma}{dxdy})^{\bar{\nu}_\mu N}_{NC}}{\int dxdy(\frac{d\sigma}{dxdy})^{\bar{\nu}_\mu N}_{CC}} \qquad (II.26b)$$

$$r = \frac{\int dxdy(\frac{d\sigma}{dxdy})^{\bar{\nu}_\mu N}_{CC}}{\int dxdy(\frac{d\sigma}{dxdy})^{\nu_\mu N}_{CC}} \qquad (II.26c)$$

then one can rewrite the Llewellyn Smith relations as:

$$R_\nu = \rho^2\left\{\left[\frac{1}{2} - \sin^2\Theta_W\right] + \frac{5}{9}\sin^4\Theta_W\left[1 + r\right]\right\} \qquad (II.27)$$

$$R_{\bar{\nu}} = \rho^2\left\{\left[\frac{1}{2} - \sin^2\Theta_W\right] + \frac{5}{9}\sin^4\Theta_W\left[1 + r^{-1}\right]\right\} \qquad (II.28)$$

We see from the above that for the simplified situation of neutrino scattering off isoscalar targets, assumed to be composed only of quarks and antiquarks of the first family, one can obtain $\sin^2\Theta_W$ and ρ experimentally, provided one measures at the same time the charged and neutral current cross sections. Of course, in real life, scattering is done on not purely isoscalar targets. Furthermore, one must also take into account that nucleons have also a sea of strange quarks, charm quarks, etc. These real life effects, however, give rise to small corrections, which one can account for in a systematic way.

As an illustration of what happens in practice, I indicate briefly the procedure followed by the CDHS collaboration [11] to extract $\sin^2\Theta_W$. Analogous corrections have been also applied in other deep inelastic experiments [12,13,14]. What was measured by the CDHS collaboration are the ratios R_ν and r, with the results

$$R_\nu = 0.3072 \pm 0.0025 \pm 0.0020 \qquad (II.29)$$

$$r = 0.39 \pm 0.01 \qquad (II.30)$$

where the two errors in Eq (II.29) are, respectively, statistical and systematic. Assuming $\rho = 1$, the Llewellyn Smith relation Eq (II.27) implies a value

$$(\sin^2\Theta_W)_{uncorr.} = 0.236 \pm 0.005 \qquad (II.31)$$

To obtain a final value for the Weinberg angle, however, a number of corrections must be applied. The major "experimental" correction comes from the fact that the target, Fe, is not purely isoscalar. This lowers the value of $\sin^2\Theta_W$ by -0.009 [11]. There are, on the other hand, a number of smaller "experimental" corrections, connected with the presence of strange and charm quarks in the nucleon, which essentially cancel this shift. In addition, however, one must apply electroweak radiative corrections to the data and when this is done - in the manner which I shall explain below - one lowers $\sin^2\Theta_W$ by -0.011 [11]. In performing all of these corrections one incurs a certain theoretical error, because one needs to estimate many things which are not precisely known (e.g. the amount of strange sea). The biggest error in the final value one obtains for $\sin^2\Theta_W$ is due to the uncertainty in the value of the charm quark mass, which affects particularly the ratio r. Carrying through all these corrections CDHS obtains finally a value for $\sin^2\Theta_W$:

$$\sin^2\Theta_W = 0.225 \pm 0.005 \pm [0.003 \pm 0.013(m_c - 1.5\ GeV)] \qquad (II.32)$$

The error in the square bracket is an estimate of the theoretical uncertainty. Assuming, as is reasonable, that $m_c = 1.5 \pm 0.3\ GeV$, then the full m_c uncertainty gives a theoretical error of [0.005]. The electroweak radiative effects included in Eq (II.32) are computed using a definition of $\sin^2\Theta_W$ in which

$$\sin^2\Theta_W = 1 - \frac{M_W^2}{M_Z^2} \qquad (II.33)$$

I will explain shortly why one needs to specify precisely what one means by $\sin^2\Theta_W$, when one computes radiative corrections. Here I note only that these radiative effects have **lowered** the raw experimental value for $\sin^2\Theta_W$ by about 4%.

The results of CDHS are in perfect agreement with results obtained at Fermilab [13,14] and by the other large neutrino scattering experiment at CERN, CHARM [12]. Assuming that $\rho = 1$, the results of all these experiments, including CDHS, are reported in Table II.1. The error in brackets in this Table is an estimate of the theoretical uncertainty.

Table II.1: Results of Deep Inelastic Neutrino Experiments for $\sin^2\Theta_W$

$\sin^2\Theta_W = 0.225 \pm 0.005 \pm [0.005]$ CDHS[11]
$\sin^2\Theta_W = 0.236 \pm 0.005 \pm [0.005]$ CHARM[12]
$\sin^2\Theta_W = 0.239 \pm 0.010$ CCFRR[13]
$\sin^2\Theta_W = 0.246 \pm 0.016$ FMM[14]

Recently a global reanalysis of these inelastic experiments, and of all other neutral current experiments, has been performed by two groups [15] [16]. I will give below, for definiteness, the results of Amaldi et al [15]. However, those of Costa et al [16] are quite similar. Correcting the raw experimental value of $\sin^2\Theta_W$ for all experimental effects, but not including radiative corrections, Amaldi et al [15] arrive at a "bare" average value for the Weinberg angle of

$$(\sin^2\Theta_W^0)_{DIS} = 0.242 \pm 0.006 \qquad (II.34)$$

Applying radiative corrections, adopting the definition Eq (II.33) for $\sin^2\Theta_W$ and using in addition the values $m_t = 45\ GeV$ and $M_H = 100\ GeV$, for the yet unknown top and Higgs masses, gives a downward shift

$$\delta s^2 = -0.009 \pm 0.001 \qquad (II.35)$$

The final value quoted by Amaldi et al [15] from their global fit of all neutrino deep inelastic data, assuming $\rho = 1$, is

$$(\sin^2\Theta_W)_{DIS} = 0.233 \pm 0.003 \pm [0.005] \qquad (II.36)$$

which is in perfect agreement with the values given by the individual experiments in Table II.1.

To determine ρ in addition one needs to measure also $R_{\bar{\nu}}$. The most accurate values for $R_{\bar{\nu}}$ come from the CERN experiments [17] [18]

$$\begin{aligned} R_{\bar{\nu}} &= 0.363 \pm 0.015 \quad CDHS\ [17] \\ R_{\bar{\nu}} &= 0.377 \pm 0.020 \quad CHARM\ [18] \end{aligned} \qquad (II.37)$$

Including also experimental information on $R_{\bar{\nu}}$, Amaldi et al [15] obtain values for both ρ and $\sin^2\Theta_W$. A two parameter fit of all data yields:

$$\sin^2\Theta_W = 0.232 \pm 0.014 \pm [0.008] \qquad (II.38)$$

$$\rho = 0.999 \pm 0.013 \pm [0.008] \qquad (II.39)$$

One sees that the above is quite consistent with the fit obtained by fixing $\rho = 1$. Furthermore, Eq (II.39) shows that the hypothesis of doublet Higgs breaking is well established experimentally.

II.2 Interference Experiments in Deep Inelastic Scattering

The effects of the weak neutral current are also detectable in charged lepton deep inelastic scattering: $\ell^\pm N \to \ell^\pm X$. These processes in the parton model, involve both γ and Z

exchange between the incident leptons and the constituent quarks, as shown in Fig. II.3.

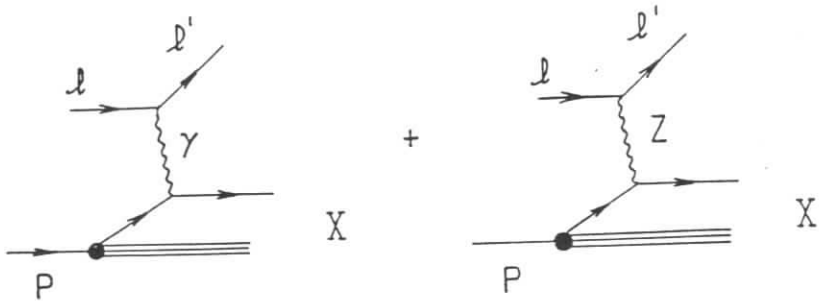

Fig. II.3: NC Contributions to deep inelastic lepton scattering

To compute the hadronic cross section one must add the γ and Z contributions at the parton level in amplitude, which leads to an interference effect between these two contributions. For $q^2 << M_Z^2$, the leading weak interaction corrections to these dominant electromagnetic processes are contained in these interference terms. Schematically, one has for the total amplitude

$$\begin{aligned} |T|^2 &= |T_\gamma + T_Z|^2 \underset{q^2 << M_Z^2}{\sim} |\frac{e^2}{q^2} + G_F|^2 \\ &\simeq |T_\gamma|^2 \left\{ 1 + \frac{q^2 G_F}{e^2} \right\} \end{aligned} \qquad (II.40)$$

Clearly the weak effects are small, at moderate q^2, being of order $10^{-4} q^2$ (GeV^2). Thus to observe these corrections experimentally, one must get rid of the dominant γ- exchange terms in (II.40). This is readily done by studying some asymmetry.

It is easy to convince oneself that there are three different types of asymmetry measurements one can preform, with a total of four possible distinct measurements. These possibilities are directly correlated with the helicities and charges of the incident leptons. One has either a

i) Polarization asymmetry

$$A^{\pm} = \frac{d\sigma_{\ell_R^{\pm}} - d\sigma_{\ell_L^{\pm}}}{d\sigma_{\ell_R^{\pm}} + d\sigma_{\ell_L^{\pm}}} \qquad (II.41)$$

or a

ii) Mixed asymmetry

$$B_{R,L} = \frac{d\sigma_{\ell^+_{R,L}} - d\sigma_{\ell^-_{L,R}}}{d\sigma_{\ell^+_{R,L}} + d\sigma_{\ell^-_{L,R}}} \qquad (II.42)$$

or a

iii) Charge asymmetry

$$C_{R,L} = \frac{d\sigma_{\ell^+_{R,L}} - d\sigma_{\ell^-_{R,L}}}{d\sigma_{\ell^+_{R,L}} + d\sigma_{\ell^-_{R,L}}} \qquad (II.43)$$

Experimentally, only two of the above asymmetries have been studied: A^- has been measured at SLAC in polarized electron deuteron deep inelastic scattering [19], while B_R has been measured at CERN by scattering polarized muons on ^{12}C [20].

The calculation of the asymmetries for the various deep inelastic processes follows directly from the effective Lagrangian in momentum space which describe the interactions shown in Fig. II.3. For $q^2 << M_Z^2$, the Z exchange term can be taken in the Fermi approximation and one has, for electron scattering,

$$\mathcal{L}_{eff}(q^2) = \frac{4\pi\alpha}{q^2} (J^\mu_{em})_e (J^{em}_\mu)_q + \sqrt{2} G_F \rho (J^\mu_{NC})_e (J^{NC}_\mu)_q \qquad (II.44)$$

It is convenient to write the above in a helicity basis which yields

$$\begin{aligned} \mathcal{L}_{eff}(q^2) = &-\frac{4\pi\alpha}{q^2} \left[\bar{e}_R \gamma^\mu e_R + \bar{e}_L \gamma^\mu e_L \right] Q_q \left[\bar{q}_R \gamma_\mu q_R + \bar{q}_L \gamma_\mu q_L \right] \\ &+ 4\sqrt{2} G_F \rho \left[Q_e^R \bar{e}_R \gamma^\mu e_R + Q_e^L \bar{e}_L \gamma^\mu e_L \right] \cdot \\ &\cdot \left[Q_q^R \bar{q}_R \gamma_\mu q_R + Q_q^L \bar{q}_L \gamma_\mu q_L \right] \end{aligned} \qquad (II.45)$$

The computation of the relevant cross section is immediate by using Eq (II.8), which detail the y-dependence of the various helicity cross sections for particle-particle scattering. For antiparticle-particle scattering, as we indicated in (II.19), one just interchanges the roles of the left and right helicities. Using these results one finds for electron or positron scattering on a right handed quark the following differential cross sections:

$$d\sigma_{e_R^-}(q_R) \sim |-\frac{\pi\alpha}{q^2}Q_q + \sqrt{2}G_F\rho Q_e^R Q_q^R|^2 \qquad (II.46a)$$

$$d\sigma_{e_L^-}(q_R) \sim |-\frac{\pi\alpha}{q^2}Q_q + \sqrt{2}G_F\rho Q_e^L Q_q^R|^2(1-y)^2 \qquad (II.46b)$$

$$d\sigma_{e_R^+}(q_R) \sim |-\frac{\pi\alpha}{q^2}Q_q + \sqrt{2}G_F\rho Q_e^L Q_q^R|^2 \qquad (II.46c)$$

$$d\sigma_{e_L^+}(q_R) \sim |-\frac{\pi\alpha}{q^2}Q_q + \sqrt{2}G_F\rho Q_e^R Q_q^R|^2(1-y)^2 \qquad (II.46d)$$

while for the scattering off a left handed quark one has

$$d\sigma_{e_R^-}(q_L) \sim |-\frac{\pi\alpha}{q^2}Q_q + \sqrt{2}G_F\rho Q_e^R Q_q^L|^2(1-y)^2 \qquad (II.47a)$$

$$d\sigma_{e_L^-}(q_L) \sim |-\frac{\pi\alpha}{q^2}Q_q + \sqrt{2}G_F\rho Q_e^L Q_q^L|^2 \qquad (II.47b)$$

$$d\sigma_{e_R^+}(q_L) \sim |-\frac{\pi\alpha}{q^2}Q_q + \sqrt{2}G_F\rho Q_e^L Q_q^L|^2(1-y)^2 \qquad (II.47c)$$

$$d\sigma_{e_L^+}(q_L) \sim |-\frac{\pi\alpha}{q^2}Q_q + \sqrt{2}G_F\rho Q_e^R Q_q^L|^2 \qquad (II.47d)$$

Similar expressions apply also for scattering off antiquarks. However, since the effect of antiquarks is small I will, for simplicity, neglect these contributions altogether in what follows.

In this approximation, the relevant cross section which enters in the various asymmetries are just given by

$$d\sigma_{e^\pm_{R,L}}(q) = d\sigma_{e^\pm_{R,L}}(q_R) + d\sigma_{e^\pm_{R,L}}(q_L) \qquad (II.48)$$

Furthermore, if one keeps only terms of $0(G_F)$, one has

$$d\sigma_{e_R^-}(q) \sim Q_q^2\Big[1+(1-y)^2\Big] - \frac{2\sqrt{2}G_F\rho q^2}{\pi\alpha}Q_q Q_e^R\Big[Q_q^R + Q_q^L(1-y)^2\Big] \qquad (II.49a)$$

$$d\sigma_{e_L^-}(q) \sim Q_q^2\Big[1+(1-y)^2\Big] - \frac{2\sqrt{2}G_F\rho q^2}{\pi\alpha}Q_q Q_e^L\Big[Q_q^L + Q_q^R(1-y)^2\Big] \qquad (II.49b)$$

$$d\sigma_{e_R^+}(q) \sim Q_q^2\Big[1+(1-y)^2\Big] - \frac{2\sqrt{2}G_F\rho q^2}{\pi\alpha}Q_q Q_e^L\Big[Q_q^R + Q_q^L(1-y)^2\Big] \qquad (II.49c)$$

$$d\sigma_{e_L^+}(q) \sim Q_q^2\Big[1+(1-y)^2\Big] - \frac{2\sqrt{2}G_F\rho q^2}{\pi\alpha}Q_q Q_e^R\Big[Q_q^L + Q_q^R(1-y)^2\Big] \qquad (II.49d)$$

If one considers scattering of polarized leptons on isoscalar targets $N = \frac{1}{2}(n+p)$ then, effectively, matters simplify further. Considering only the quarks of the 1^{st} generation, one has

$$\sum_q q(x,q^2)d\sigma(q) \to \frac{1}{2}\Big[u(x,q^2)+d(x,q^2)\Big]\Big\{d\sigma(u)+d\sigma(d)\Big\} \qquad (II.50)$$

In this case, clearly, the asymmetries A, B, C are independent of the structure functions and just follow from the asymmetries at the quark level.

For the A^- asymmetry measured at SLAC, in particular, one finds

$$A^- = \frac{d\sigma_{e_R^-} - d\sigma_{e_L^-}}{d\sigma_{e_R^-} + d\sigma_{e_L^-}} = -\frac{G_F\rho q^2}{\sqrt{2}\pi\alpha}\left[\frac{\sum_q Q_q(\alpha_q + \beta_q f(y))}{\sum_q Q_q^2}\right] \qquad (II.51)$$

where

$$f(y) = \frac{1-(1-y)^2}{1+(1-y)^2} \qquad (II.52)$$

and

$$\begin{aligned}\alpha_q &= \Big(Q_e^R - Q_e^L\Big)\Big(Q_q^R + Q_q^L\Big)\\ \beta_q &= \Big(Q_e^R + Q_e^L\Big)\Big(Q_q^R - Q_q^L\Big)\end{aligned} \qquad (II.53)$$

Note that both the coefficient α_q and β_q are parity violating – either at the electron or at the quark vertex. In terms of $\sin^2\Theta_W$ and ρ one finds for A^- the explicit expression

$$A^- = -\frac{G_F\rho q^2}{\sqrt{2}\pi\alpha}\left[\left(\frac{9}{20} - \sin^2\Theta_W\right) + \left(\frac{9}{20} - \frac{9}{5}\sin^2\Theta_W\right)f(y)\right] \qquad (II.54)$$

This asymmetry was measured in a classic experiment by a SLAC-Yale group about 10 years ago [19]. The data, shown in Fig. II.4, shows little y-dependence, indicating that $\sin^2\Theta_W \simeq \frac{1}{4}$. Assuming that $\rho = 1$, the magnitude of the asymmetry then fixes $\sin^2\Theta_W$ itself. The result obtained [19]

$$\sin^2\Theta_W = 0.224 \pm 0.012 \pm 0.008 \qquad (II.55)$$

where the first error above is statistical and the second is systematic, is in a perfect agreement with the results for $\sin^2\Theta_W$ obtained in deep inelastic neutrino experiments.

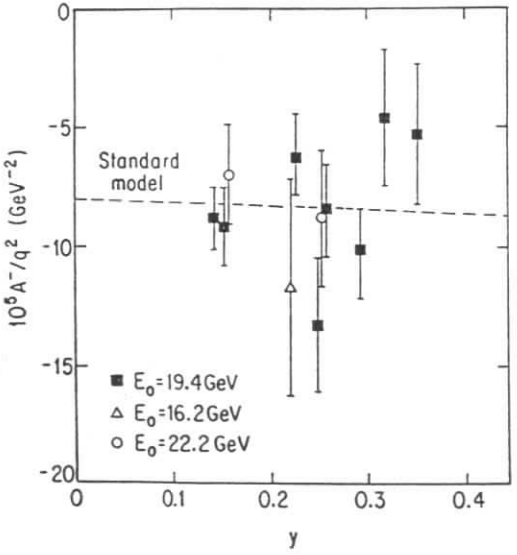

Fig. II.4: Polarized asymmetry A^-/q^2 measured by the SLAC-Yale experiment [19] as a function of y.

A few remarks are in order:

i) The SLAC-Yale experiment [19] provides an important confirmation of the validity of the standard model, since what is measured here are different neutral current vertices

than those entering in neutrino experiments. In the standard model these vertices are all related to $\sin^2\Theta_W$, so that obtaining the same $\sin^2\Theta_W$ from these different experiments does give an important cross check of the model.

ii) The result given in (II.55) does not include radiative corrections. These typically [15] lower the value of $\sin^2\Theta_W$ in Eq (II.55) by about 0.01, which is within the quoted experimental errors.

iii) The theoretical corrections to the formula (II.51) [or (II.54)] for A^- are rather small. For instance, incorporating the neglected antiquark contributions replaces the coefficient of $f(y)$ in these expressions by

$$f(y) \to \left[\frac{q(x;q^2) - \bar{q}(x;q^2)}{q(x,q^2) + \bar{q}(x,q^2)}\right] f(y) \qquad (II.56)$$

where $q(x;q^2) = u(x;q^2) + d(x;q^2)$. The above is actually a rather small correction since, for the moderate values of x relevant to the SLAC experiment, the antiquark distributions are just a small fraction of those of the quarks.

The BCDMS collaboration at CERN [20] has measured the mixed asymmetry B_R using polarized $\mu^\pm$ beams interacting on a ^{12}C target. A similar calculation to the one above gives, in the standard model, the following result for this asymmetry:

$$\begin{aligned} B_R = \frac{d\sigma_{\mu_R^+} - d\sigma_{\mu_L^-}}{d\sigma_{\mu_R^+} + d\sigma_{\mu_L^-}} &= -\frac{\sqrt{2}G_F\rho q^2}{\pi\alpha} f(y) \frac{\sum_q Q_q Q_e^L (Q_q^R - Q_q^L)}{\sum_q Q_q^2} \\ &= -\frac{9G_F\rho}{10\sqrt{2}\pi\alpha}(1 - 2\sin^2\Theta_W) f(y) q^2 \equiv b f(y) q^2 \end{aligned} \qquad (II.57)$$

Note that since $B_R \sim Q_e^L(Q_q^R - Q_q^L)$, this asymmetry is not a purely parity violating asymmetry. Because of this, when one compares (II-57) to experiment it is necessary to subtract from the data purely electromagnetic $0(\alpha^3)$ corrections, which do give a non zero contribution to B_R.

Using $\sin^2\Theta_W = 0.23$, $\rho = 1$, Eq (II.57) predicts for the slope parameter b the value:

$$b^{GSW} = -1.51 \times 10^{-4} GeV^{-2} \qquad (II.58)$$

The experimental data for B_R, corrected for purely eletromagnetic effects, is plotted versus $f(y)\ q^2$ in Fig. II.5. The slope parameters for the two energies measured are, within errors, in perfect agreement with this prediction:

$$\begin{aligned} b(120\ GeV) &= (-1.76 \pm 0.75) \times 10^{-4} GeV^{-2} \\ b(200\ GeV) &= (-1.47 \pm 0.37) \times 10^{-4} GeV^{-2} \end{aligned} \qquad (II.59)$$

The errors, however, are too large to use this data to get a stringent value for $\sin^2\Theta_W$.

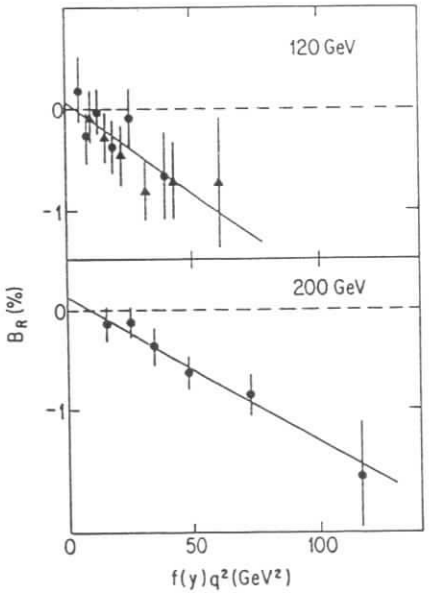

Fig II.5: q^2 dependence of the B_R asymmetry from [20]

II.3 Detection of $W^{\pm}$ and Z and Radiative Corrections

Perhaps the most impressive confirmation of the standard model was provided by the $UA1$ and $UA2$ collaborations working at the CERN $p\bar{p}$ collider, by detecting the weak bosons $W^{\pm}$ and Z, with the masses predicted by the model [21] [22]. Recalling the formulas

$$\frac{G_F}{\sqrt{2}} = \frac{e^2}{8 \sin^2\Theta_W M_W^2}, \qquad (II.60)$$

coming from the Fermi theory comparison, and

$$\frac{M_W^2}{M_Z^2 \cos^2\Theta_W} = \rho = 1, \qquad (II.61)$$

coming from doublet Higgs breaking, and using $\sin^2\Theta_W = 0.23$ yields

$$M_W = 77.8\ GeV; \quad M_Z = 88.7\ GeV \qquad (II.62)$$

These values are in good agreement with the mass values measured for the W and Z bosons by the $UA1$ and $UA2$ collaborations, as can be gathered from Table II.2 which contains a recent compilation of these results [23]

Table II.2: Values of W and Z Masses [23]

$M_W = (82.7 \pm 1.0 \pm 2.7)$ GeV UA1$(e\nu)$	Average
$M_W = (80.2 \pm 0.6 \pm 1.7)$ GeV UA2$(e\nu)$	$M_W = (80.8 \pm 1.3)$ GeV
$M_Z = (93.1 \pm 1.0 \pm 3.1)$ GeV UA1(e^+e^-)	Average
$M_Z = (91.5 \pm 1.2 \pm 1.7)$ GeV UA2(e^+e^-)	$M_Z = (92.0 \pm 1.8)$ GeV

Although the agreement of theory with the experimental results is impressive at first sight, both the W and Z masses appear to be a few GeV higher than the values given in Eq

(II.62). One must realize, however, that if one wants to check the predictions of the model to the percent accuracy, one must worry about the effect of electroweak radiative corrections. It turns out that when one incorporates these radiative effects both the W and Z mass values predicted by the theory are raised, thereby improving the agreement with experiment. Let me discuss this important point.

I have indicated briefly earlier than when considering radiative corrections one must specify how $\sin^2\Theta_W$ is defined. In the 0^{th} order discussion of Sec.I we have defined $\sin^2\Theta_W$ in a number of different - but to this order, equivalent - ways:

i) Through the unification condition, Eq (I.8):

$$e = g'\cos\Theta_W = g\sin\Theta_W \qquad (II.63)$$

ii) Via the interrelation of the W and Z masses, corresponding to doublet Higgs breaking, Eq (I.27):

$$\sin^2\Theta_W = 1 - \frac{M_W^2}{M_Z^2} \qquad (II.64)$$

iii) By comparing the low energy charged current interactions with the Fermi theory, Eq (I.15):

$$\frac{G_F}{\sqrt{2}} = \frac{e^2}{8\sin^2\Theta_W M_W^2} \qquad (II.65)$$

iv) From the structure of the neutral current itself, Eq (I.19):

$$J^\mu_{NC} = 2(J^\mu_3 - \sin^2\Theta_W J^\mu_{em}) \qquad (II.66)$$

Although these ways of specifying the Weinberg angle are equivalent in lowest order in α, each of these definitions will get different corrections in higher order, with the corrections depending precisely on how the Weinberg angle is physically defined. Thus one must agree on some definition of $\sin^2\Theta_W$, and then all other definitions will be related in a calculable way to this conventionally picked value.

Most useful is to focus on some expression which relates $\sin^2\Theta_W$ to some measurable quantity. For instance, the $\sin^2\Theta_W$ that enters in the definition of J^μ_{NC} implies, at lowest order, the expression (II.10) for the ratio R of the $\nu_\mu e$ to $\bar{\nu}_\mu e$ cross sections, which is purely a function of $\sin^2\Theta_W$. Consider, however, this same ratio in higher order. At $0(\alpha)$ one needs to add many more graphs to $\nu_\mu e$ scattering, as shown schematically in Fig. II.6

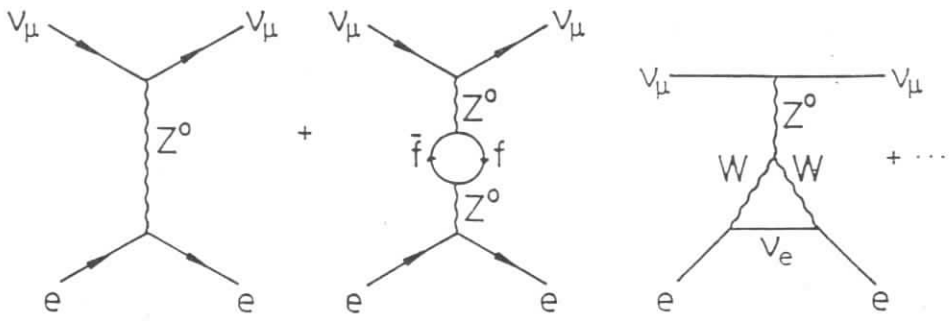

Fig. II.6: Corrections to $\nu_\mu e$ scattering to $0(\alpha)$

These $0(\alpha)$ contributions are singular, but the infinities appearing in R can be reabsorbed into redefinitions of the coupling constants and of $<\Phi>$. Depending on how one does this renormalization process one arrives at different definitions of the renormalized $\sin^2\Theta_W$. In particular, one could define this renormalized $\sin^2\Theta_W$ [called $\sin^2\Theta^R_W$ below] by the demand that the $0(\alpha)$ expression for R be precisely the same as the lowest order expression. That is, to $0(\alpha)$

$$R|_{0(\alpha)} = \frac{3 - 12\sin^2\Theta^R_W + 16\sin^4\Theta^R_W}{1 - 4\sin^2\Theta^R_W + 16\sin^4\Theta^R_W} \qquad (II.67)$$

This equation then fixes how the Weinberg angle is defined in all other $0(\alpha)$ computations. For instance, for the mass shifts to the W and Z masses, coming through the vacuum polarization graphs of Fig. II.7 one now has a fixed prescription on how the infinities are reabsorbed. Reabsorbing these infinities with $\sin^2\Theta^R_W$ defined via Eq (II.67), one finds

$$1 - \frac{M_W^2}{M_Z^2} = \sin^2\Theta^R_W[1 + C\alpha] \qquad (II.68)$$

with C some calculable finite number *

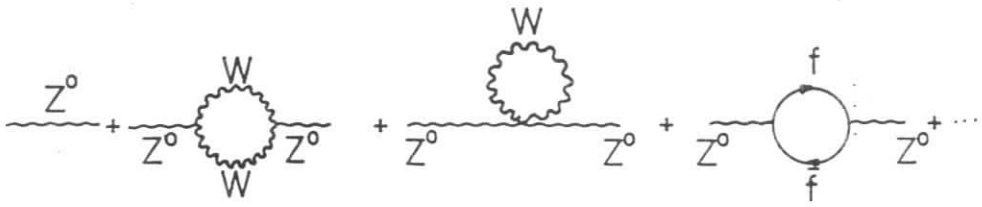

Fig. II.7: Vacuum polarization graphs giving mass shifts to the weak boson masses

Of course, one could have done this differently and defined the Weinberg angle to $0(\alpha)$ through the mass ratio

$$1-\frac{M_W^2}{M_Z^2}\,|_{0(\alpha)} \equiv (\sin^2\Theta_W)^{mass} \qquad (II.69)$$

With this definition, obviously the expression for R would differ from the lowest order value. Indeed using (II.68), one sees that

$$R=\frac{3-12(\sin^2\Theta_W)^{mass}+16(\sin^4\Theta_W)^{mass}+\alpha C[-12+32(\sin^2\Theta_W)^{mass}]}{1-4(\sin^2\Theta_W)^{mass}+16(\sin^4\Theta_W)^{mass}+\alpha C[-4+32(\sin^2\Theta_W)^{mass}]} \qquad (II.70)$$

It is most convenient to use $(\sin^2\Theta_W)^{mass}$ as a definition of the renormalized Weinberg angle. Henceforth we shall adopt this definition and drop the superscript mass, so that

$$(\sin^2\Theta_W)^{mass} \equiv \sin^2\Theta_W = 1-\frac{M_W^2}{M_Z^2} \qquad (II.71)$$

* Keeping only the leading logarithmic terms one finds $C\alpha \simeq -\frac{\alpha}{\pi} ln \frac{M_W^2}{m_q^2}$ [24]

This definition, which was suggested by Sirlin [25], is particularly useful in that one can estimate the radiative corrections by means of the renormalization group [24]. Furthermore, it is this definition of $\sin^2\Theta_W$ which has been used in computing the radiative corrections for the deep inelastic neutrino scattering experiments, reported in Sec II.1.

One potential way to test these radiative effects would be to compute $\sin^2\Theta_W$ from the value of the W and Z masses measured at the CERN collider, and compare this value with that obtained in deep inelastic scattering. Unfortunately, although systematic errors cancel mostly in the ratio, the statistical errors remaining are too big for a meaningful comparison. Averaging the $UA1$ and $UA2$ data one finds

$$\sin^2\Theta_W = 1-\frac{M_W^2}{M_Z^2} = 0.222 \pm 0.018, \qquad (II.72)$$

which agrees within errors with the value of $\sin^2\Theta_W$ obtained in deep inelastic scattering, Eq (II.36). However, it also agrees within errors with the "bare" value $[(\sin^2\Theta_W^0)_{DIS} = 0.242 \pm 0.006]$ computed without doing any radiative corrections.

One can do a more meaningful comparison by looking directly at a modified formula for M_W, including radiative corrections. With the definition of $\sin^2\Theta_W$ of (II.71), the lowest order relation obtained from the Fermi theory comparison [Eq (I.15)] between M_W^2 and $\sin^2\Theta_W$ gets modified to

$$M_W^2 = \frac{\pi\alpha}{\sqrt{2}G_F\sin^2\Theta_W}\left[\frac{1}{1-\Delta r}\right] \qquad (II.73)$$

In the above α is the fine structure constant, $\alpha = \frac{e^2}{4\pi}$, measured at zero momentum transfer, while G_F is the Fermi constant measured in muon decay (with certain small electromagnetic corrections included [26]). Both these parameters are known to high accuracy. The factor in the square bracket is a theoretically computable radiative correction [27], which for the definition of $\sin^2\Theta_W$ adopted is rather large. Δr, however, does depend (slightly) on the values adopted for the two unknown parameters of the 3 generation standard model, m_t and M_H. Using as canonical values $m_t = 45\ GeV$ and $M_H = 100\ GeV$, one finds [15] [27]*

$$\Delta r = 0.0713 \pm 0.013 \qquad (II.74)$$

* The error is due to uncertainties in the value of the low energy $e^+e^- \to$ hadron cross section needed to fully estimate Δr.

The radiative correction changes the numerical relation between M_W^2 and $\sin^2\Theta_W$ from that of the simple Fermi theory comparison. One has

$$M_W^2 = \frac{(37.281\ GeV)^2}{\sin^2\Theta_W[1-\Delta r]} = \frac{(38.685\ GeV)^2}{\sin^2\Theta_W} \qquad (II.75)$$

Using the $UA1$ and $UA2$ vector boson masses in Table II.2, one obtains an average value of $\sin^2\Theta_W$ - including also an estimate of the possible theoretical uncertainty (given in square brackets) - of

$$(\sin^2\Theta_W)_{W/Z} = 0.228 \pm 0.007 \pm [0.002] \qquad (II.76)$$

This value is in excellent agreement with the value of $\sin^2\Theta_W$ obtained in deep inelastic scattering [Eq (II.36)].

$$(\sin^2\Theta_W)_{DIS} = 0.233 \pm 0.003 \pm [0.005] \qquad (II.77)$$

Conversely, if one uses the value for $\sin^2\Theta_W$ found in deep inelastic scattering in the radiatively corrected formula for the W mass, one finds

$$M_W = 80.14 \pm 0.50 \pm [0.85]\ GeV \qquad (II.78)$$

This value is also in excellent agreement with the mass values observed by the $UA1$ and $UA2$ collaborations, given in Table II.2. Radiative corrections have provided about a 2.5 GeV upward shift to the "zero" order mass prediction (II.62).

One should note that the radiative shift for $(\sin^2\Theta_W)_{W/Z}$ is large and increases the bare prediction

$$(\sin^2\Theta_W^0)_{W/Z} = 0.212 \pm 0.007 \qquad (II.79)$$

to the value given in Eq. (II.76). For the case of deep inelastic scattering, this radiative shift is smaller in magnitude but opposite in sign. That is, the bare value of $\sin^2\Theta_W$ is

larger than the radiatively corrected value. So radiative corrections really do help! This is, illustrated pictorially in Fig. II.8.

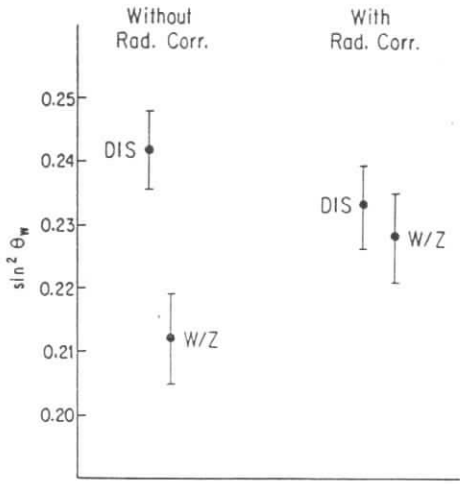

Fig. II.8: Effects of radiative corrections on $\sin^2\Theta_W$.

The result of the combined analysis of all neutral current experiments by Amaldi et al [15] gives a best value for the Weinberg angle, when $\rho = 1$, of

$$\sin^2\Theta_W = 0.230 \pm 0.0438 \qquad (II.80)$$

If ρ is allowed to vary also, the best values are

$$\begin{aligned} \sin^2\Theta_W &= 0.229 \pm 0.0064 \\ \rho &= 0.998 \pm 0.0086 \end{aligned} \qquad (II.81)$$

A graphical representation of these results (at 90% C.L.) is shown in Fig. II.9, which clearly indicates the importance of the neutrino deep inelastic experiments and of the W/Z mass

determinations for an accurate determination of $\sin^2\Theta_W$ and ρ. Note that Eq. (II.81) confirms doublet Higgs breaking to the percent level.

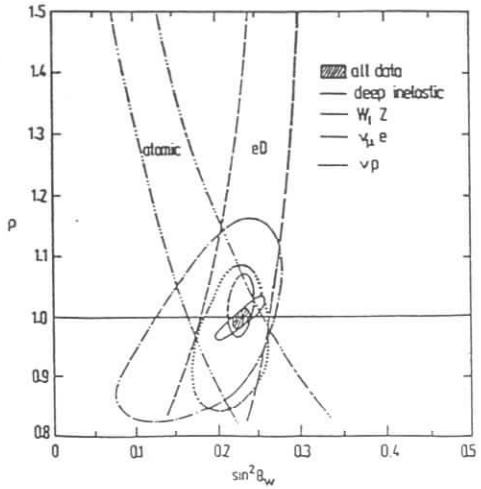

Fig. II.9: 90% C.L. confidence limits for $\sin^2\Theta_W$ and ρ, from the analysis of Amaldi et al [15].

III. FORTHCOMING TESTS OF THE ELECTROWEAK THEORY

The $SU(2) \times U(1)$ model of Glashow Salam and Weinberg [1] will get a more thorough probing with the forthcoming generation of accelerators, particularly the large e^+e^- colliders LEP and SLC. In this section, I want to discuss some of the interesting tests of the standard model which will be performed in the near future with these machines.

III.1 Precision Electroweak Tests at the Z

It is obviously very important to establish the correctness of the standard electroweak theory, including radiative corrections. We just saw that one is beginning to do this by

using the combination of deep inelastic neutrino data with the collider measurements of the W and Z masses [cf Fig. II.8]. However, the errors are still large, and one is just beginning to test for these effects. One would very much like to have, for the standard electroweak theory, a check of the radiative corrections which is equivalent to the famous $g-2$ check for QED.

One such test is provided by the radiative correction Δr, introduced in Eq (II.73). One may rewrite this equation, using the numerical values for G_F and α, in a number of alternate ways, by exploiting the interrelation between $\sin^2\Theta_W, M_W^2$ and M_Z^2 of the defining equation (II.71):

$$1-\Delta r = \frac{(37.281\ GeV)^2}{M_W^2 \sin^2\Theta_W} = \frac{(37.281\ GeV)^2 M_Z^2}{M_W^2(M_Z^2-M_W^2)} = \frac{(37.281\ GeV)^2}{M_Z^2 \sin^2\Theta_W \cos^2\Theta_W} \qquad (III.1)$$

Eq (III.1) makes it clear that a careful measurement of either of the following pairs of quantities: $(M_W^2, \sin^2\Theta_W)$; (M_W^2, M_Z^2); or $(M_Z^2, \sin^2\Theta_W)$ will fix $(\Delta r)_{exp}$ and permit an accurate comparison with the theoretical value (II.74).

At the moment, however, one does not have the possibility of performing a very accurate test of this theoretical prediction. Using the value of the Weinberg angle obtained in deep inelastic scattering, Eq (II.77) [$\sin^2\Theta_W = 0.233 \pm 0.003 \pm [0.005]$] and the average value for the W mass given in Table II.2 [$M_W = 80.8 \pm 1.3\ GeV$], one deduces that

$$(\Delta r)_{exp} = 0.09 \pm 0.04 \qquad (III.2)$$

This value is indeed in perfect agreement with the theoretical prediction given in Eq (II.74). However, the accuracy is such that $(\Delta r)_{exp}$ is a bit more than 2σ away from being zero. As I will discuss below, measurements at LEP and SLC will be able to considerably reduce the error on Δr and thus provide a much more meaningful test of the radiative corrections.

Before discussing these precision tests, it is useful to try to understand theoretically why Δr is so large ($\Delta r \sim 7\%$) and to try to describe how the theoretical value depends on the

unknown parameters m_t and M_H in the standard model. The magnitude of the correction Δr can be readily understood physically [24]. In Eq (II.73) two of the parameters α and G_F are specified from experiments done at low q^2. On the other hand, M_W^2 and $\sin^2\Theta_W$ are quantities that involve a scale of $0(100GeV)$. Radiative corrections can only be large if there are large logarithms: $\frac{\alpha}{\pi} ln \frac{M_W^2}{<q^2>}$, since α itself is a small parameter. This suggests [24] that if one replaces α and G_F in Eq (II.73) by their running values, $\alpha(M_W^2)$ and $G_F(M_W^2)$, since all quantities are now evaluated at the same scale, the bulk of the radiative effects should be accounted for. That is, one expect that including radiative corrections [24],

$$M_W^2 = \frac{\pi\alpha}{\sqrt{2}G_F \sin^2\Theta_W[1-\Delta r]} \simeq \frac{\pi\alpha(M_W^2)}{\sqrt{2}G_F(M_W^2)\sin^2\Theta_W} \qquad (III.3)$$

The computation of the running of α is through the usual QED vacuum graphs, involving all the fermions entering in the theory, leading to the familiar result

$$\alpha(M_W^2) = \frac{\alpha}{1 - \frac{\alpha}{3\pi}\sum_f Q_f^2 ln \frac{M_W^2}{m_f^2}} \qquad (III.4)$$

The uncertainties in the light quark masses entering in this formula can be largely avoided by using the low energy e^+e^- annihilation experimental cross sections [24]. Furthermore, the error arising from not knowing the value of the top quark mass is not very large. A direct evaluation gives

$$\alpha(M_W^2) \simeq \frac{1}{128} \qquad (III.5)$$

It turns out that the Fermi constant above, which is measured in μ-decay, does not run. Thus $G_F(M_W^2) \simeq G_F$. This last point can be understood as follows. The effective Lagrangian for μ decay can be rewritten by means of a Fierz transformation into a product of a neutrino current times a charged lepton current

$$\begin{aligned} \mathcal{L}_{eff} &= \frac{G_F}{\sqrt{2}}[\bar{\mu}\gamma^\alpha(1-\gamma_5)\nu_\mu][\bar{\nu}_e\gamma_\alpha(1-\gamma_5)e] \\ &= \frac{G_F}{\sqrt{2}}[\bar{\mu}\gamma^\alpha(1-\gamma_5)e][\bar{\nu}_e\gamma_\alpha(1-\gamma_5)\nu_\mu] \end{aligned} \qquad (III.6)$$

Now $G_F(M_W^2)$ is a modification of the usual Fermi constant, coming from logarithmic virtual photon corrections. These corrections, in the language of the renormalization group,

give rise to an anomalous dimension for the μ decay operator in (III.6). However, the currents entering in the second line of Eq (III.6) are really very special. The neutrino current is inert under electromagnetism, while the $e-\mu$ current is conserved, and thus has no anomalous dimension [24]. Hence $G_F(M_W^2) = G_F$.

Using the above results, one can rewrite the formula for Δr coming from Eq (III.3) as

$$1 - \Delta r \simeq \frac{\alpha}{\alpha(M_W^2)} \frac{G_F(M_W^2)}{G_F} \simeq \frac{\alpha}{\alpha(M_W^2)} \simeq \frac{128}{137} = 0.934 \qquad (III.7)$$

which is very close to the calculated answer. Thus one understands directly the main effect, in a qualitative fashion.

The actual number for Δr given in Eq (II.74), took as canonical values $m_t = 45\ GeV$ and $M_H = 100\ GeV$, for the two still unknown parameters in the standard model. It is important to ask how sensitively does this number depend on these choices. One finds from detailed calculations [27] [24] that Δr is quite sensitive to m_t, if $m_t \geq m_W$, but rather insensitive to M_H. Indeed, the variation of Δr with M_H is only logarithmical, while its dependence on m_t is quadratic. Numerically, one finds that [27] [24]

$$(\Delta r)_{top} \simeq 6.3 \times 10^{-3} \left(\frac{m_t}{M_W}\right)^2 \qquad (III.8)$$

while

$$(\Delta r)_{Higgs} \sim 2.3 \times 10^{-3} ln \frac{M_H^2}{M_Z^2} \qquad (III.9)$$

Using the above, one sees that even for a 1 TeV Higgs the change in Δr is small ($\delta\Delta r \sim 0.01$). On the other hand, for a 200 GeV top the predicted value for Δr is reduced to about $\Delta r \simeq 0.4$ and is 1σ away from the experimentally deduced value of Eq (III.2). Amaldi et al [15] have studied a whole gamut of neutral current processes as a function of m_t and by demanding agreement between theory and experiment obtain a 90% C.L. upper bound on m_t. Their bound depends slightly on M_H, but lies in the vicinity of 180 - 200 GeV. Clearly, if one could reduce the errors on Δr from experiment, one could narrow the range

allowed for m_t in the standard model.* Furthermore, as even large variations of M_H give at most changes in Δr at the percent level, a worthwhile goal is to try to measure Δr to this level.

Precise studies at SLC and LEP can achieve this level of accuracy [$\delta\Delta r \leq 0.01$], through a careful measurement of $\sin^2\Theta_W$. In these e^+e^- colliders, the Z mass should be measured to the per mil accuracy ($\delta M_Z \leq 100\ MeV$). Obviously, therefore, the relevant formula for extracting Δr is one in which the Z mass and $\sin^2\Theta_W$ are involved.

$$1 - \Delta r = \frac{\pi\alpha}{\sqrt{2}G_F \sin^2\Theta_W \cos^2\Theta_W M_Z^2} \qquad (III.10)$$

Neglecting the errors due to the Z mass measurement, which are tiny anyway, one sees that

$$\delta\Delta r \simeq \frac{8}{3}\delta \sin^2\Theta_W \qquad (III.11)$$

Hence to measure Δr to an accuracy of $\delta\Delta r \simeq 0.01$, requires measuring $\sin^2\Theta_W$ to $\delta\sin^2\Theta_W \simeq 0.004$. This is the present experimental accuracy for $\sin^2\Theta_W$ in deep inelastic scattering [c.f. Eq (II.36)]. However, in this case one has an additional theoretical error, coming from uncertainties in the parton model, of $\delta(\sin^2\Theta_W)^{\nu_\mu N}_{theory} = 0.005$.

At LEP/SLC one can achieve the above accuracy in $\sin^2\Theta_W$ by measuring the forward-backward asymmetry in the process $e^+e^- \to \mu^+\mu^-$ at resonance. This process receives contributions from both a γ exchange and a Z exchange graph, as shown in Fig. III.1

* There is an experimental lower bound on m_t from $UA1$ [28], $m_t \geq 44 - 56$ GeV, with the range depending on certain theoretical uncertainties for t-production in hadronic processes.

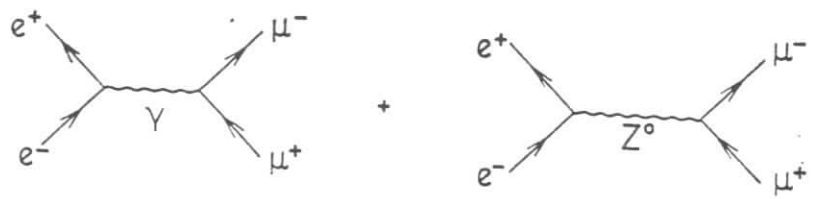

Fig. III.1: Graphs contributing, to lowest order, to the process $e^+e^- \to \mu^+\mu^-$

Using the interaction Lagrangian of the standard model, Eq (I.9), a straight forward calculation gives the following expression for the differential angular distribution for this process

$$\frac{d\sigma}{d\cos\theta} = \frac{\pi\alpha^2}{2s}\{(1+\cos^2\theta)F_1(s) + 2\cos\theta F_2(s)\} \qquad (III.12)$$

Here θ is the angle of the produced μ^- relative to the incoming e^-, while s is the CM energy squared. The functions $F_1(s)$ and $F_2(s)$ depend on the neutral current coupling of the Z to the leptons, which involve $\sin^2\Theta_W$. One finds in particular *

$$F_1(s) = 1 + \frac{2s(s-M_Z^2)}{(s-M_Z^2)^2 + M_Z^2\Gamma_{tot}^2} \cdot \frac{V_e^2}{\sin^2\Theta_W\cos^2\Theta_W} + \frac{s^2}{(s-M_Z^2)^2 + M_Z^2\Gamma_{tot}^2} \cdot \frac{(V_e^2+A_e^2)^2}{\sin^4\Theta_W\cos^4\Theta_W} \qquad (III.13a)$$

* Note that vector and axial NC couplings of the electron and the muon are the same.

and

$$F_2(s) = \frac{2s(s-M_Z^2)}{(s-M_Z^2)^2+M_Z^2\Gamma_{tot}^2}\cdot\frac{A_e^2}{\sin^2\Theta_W\cos^2\Theta_W} + \frac{4s^2}{(s-M_Z^2)^2+M_Z^2\Gamma_{tot}^2}\cdot\frac{V_e^2A_e^2}{\sin^4\Theta_W\cos^4\Theta_W} \qquad (III.13b)$$

These expressions include an explicit width for the Z boson, obtained by replacing the ordinary Feynman propagator factor $\frac{1}{M_Z^2-s}$ by $\frac{1}{M_Z^2-s-i\Gamma_{tot}M_Z}$ in the graphs of Fig. III.1. The forward-backward asymmetry is then, simply,

$$A_{FB} = \frac{\int_0^1 d\cos\theta\left(\frac{d\sigma}{d\cos\theta}\right) - \int_{-1}^0 d\cos\theta\left(\frac{d\sigma}{d\cos\theta}\right)}{\int_0^1 d\cos\theta\left(\frac{d\sigma}{d\cos\theta}\right) + \int_{-1}^0 d\cos\theta\left(\frac{d\sigma}{d\cos\theta}\right)} = \frac{3F_2(s)}{4F_1(s)} \qquad (III.14)$$

Note that A_{FB} is not a purely parity violating asymmetry, since F_2 depends on A_e^2 as well as $(A_eV_e)^2$. Thus it has purely electromagnetic $0(\alpha^3)$ contributions, which must be subtracted off before one can extract the purely weak effects from experiment.

The forward-backward asymmetry for both the $e^+e^- \to \mu^+\mu^-$ and $e^+e^- \to \tau^+\tau^-$ processes has been measured at PEP and PETRA. In this energy range, $\sqrt{s} << M_Z^2$ so that, using that $A_e = 1/4$, one has approximately

$$F_1(s) \simeq 1; \quad F_2(s) \simeq -\frac{s}{(M_Z^2-s)}\frac{1}{8\sin^2\Theta_W\cos^2\Theta_W} \qquad (III.15)$$

whence

$$A_{FB} = -\left[\frac{3}{32\sin^2\Theta_W\cos^2\Theta_W}\right]\frac{s}{M_Z^2-s} \simeq -\left[\frac{3}{32\sin^2\Theta_W\cos^2\Theta_W}\right]\frac{s}{M_Z^2} \qquad (III.16)$$

One sees from Eq (III.16) that in the PEP/PETRA range one expects A_{FB} to grow approximately linearly with s. The slope of A_{FB} vs s, in principle, depends on Θ_W. However, in practice it is quite insensitive to the Weinberg angle, since

$$\frac{1}{\sin^2\Theta_W\cos^2\Theta_W M_Z^2} = \frac{\sqrt{2}G_F}{\pi\alpha}[1-\Delta r] \qquad (III.17)$$

This linear growth is seen in Fig. III.2, taken from [29], which details the values for A_{FB} measured at PEP and PETRA. I note for later use that the best accuracy achieved so far in measuring A_{FB}, is $\delta A_{FB} \simeq 0.02$ at $\sqrt{s} = 34\ GeV$. As we shall see one will have to do better than this at LEP/SLC if one wants to extract an accurate value of $\sin^2\Theta_W$.

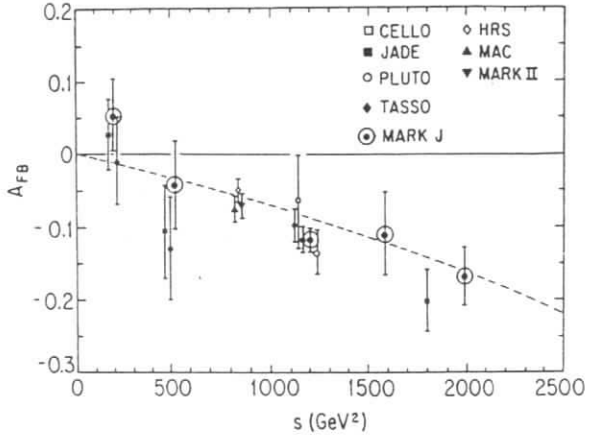

Fig. III.2: Compilation of forward-backward asymmetry measurements at PEP and PETRA, from [29].

The relevant formulas for A_{FB} change totally when one operates at $\sqrt{s} = M_Z$. In this case since $\Gamma_{tot} << M_Z$ (see below) one has

$$F_1(M_Z^2) \simeq \left(\frac{M_Z}{\Gamma_{tot}}\right)^2\frac{(V_e^2+A_e^2)^2}{\sin^4\Theta_W\cos^4\Theta_W}$$
$$F_2(M_Z^2) = 4\left(\frac{M_Z}{\Gamma_{tot}}\right)^2\frac{V_e^2A_e^2}{\sin^4\Theta_W\cos^4\Theta_W} \qquad (III.18)$$

Hence one obtains

$$A_{FB}|_{\sqrt{s}=M_Z} \simeq \frac{3V_e^2\,A_e^2}{(V_e^2+A_e^2)^2} \simeq 3(1-4\sin^2\Theta_W)^2, \qquad (III.19)$$

where use has been made that

$$V_e = \sin^2\Theta_W - \frac{1}{4} << A_e = \frac{1}{4} \qquad (III.20)$$

I note that the forward-backward asymmetry at resonance is small because $\sin^2\Theta_W \simeq \frac{1}{4}$.

One can estimate the accuracy needed on A_{FB} to get $\delta\sin^2\Theta_W \leq 0.004$, which corresponds to $\delta\Delta r \leq 0.01$. Using (III.19) and the requirement that $\delta\sin^2\Theta_W \leq 0.004$ yields the constraint:

$$\delta A_{FB} = 24[1-4\sin^2\Theta_W]\delta\sin^2\Theta_W \leq 0.1\{1-4\sin^2\Theta_W\} \qquad (III.21)$$

Thus the accuracy needed in measuring A_{FB}, to extract a useful value for $\sin^2\Theta_W$, depends on the **actual value** of this parameter *. Given the large rates at the Z, it is quite possible to imagine measuring $\sin^2\Theta_W$ to this accuracy, statistically. For instance, it has been estimated [30] that at LEP, operating at a luminosity of $10^{31}\ cm^{-2}sec^{-1}$, one could achieve a statistical error for A_{FB} of $\delta A_{FB} \leq 0.005$ in 40 days of running. However, the real trick is to maintain the systematic accuracy to this level! Furthermore, there is another complication. The measured forward-backward asymmetry has really three components

$$(A_{FB})^{exp} = A_{FB} + (A_{FB})^{EW} + (A_{FB})^{em} \qquad (III.22)$$

Only the first of these is the quantity given in Eq (II.19). The real measured asymmetry, in addition includes both electroweak radiative corrections and purely electromagnetic corrections. The first of these corrections are small compared to A_{FB}, but grow as $\sin^2\Theta_W \to 0.25$. On the other hand, the pure electromagnetic corrections are comparable in size to A_{FB}, being of the order of $2-3\%$. Furthermore, their actual value depends on the explicit experimental cuts. So to achieve a precision on A_{FB} of order 0.05% requires a

* For instance, for $\sin^2\Theta_W = 0.24$ one need $\delta A_{FB} \leq 0.004$, while for $\sin^2\Theta_W = 0.23$ one needs $\delta A_{FB} \leq 0.008$.

careful combination of both theoretical and experimental work. It will indeed be a difficult task! *

The forward-backward asymmetry A_{FB} is not the only way in which one can extract $\sin^2\Theta_W$ at the Z peak. Asymmetries involving helicity measurements, if feasible, turn out to be very good ways to try to measure $\sin^2\Theta_W$. Basically, these asymmetries require that one either have some way to polarize the initial electron and positron beams, or that one be able to detect the polarization of some finally produced state. The final state polarization asymmetry for the process $e^+e^- \to \tau^+\tau^-$, in fact, can be measured in practice by using the decay $\tau \to \pi\nu_\tau$ as a polarization analyzer. Furthermore, studies have been undertaken both at SLAC [31] and at CERN [32] to see whether one can run with longitudinally polarized e^+ and e^- beams. Although achieving polarization might be difficult - particularly at CERN where one will need spin rotators - the physics benefit of measuring initial state asymmetries for extracting $\sin^2\Theta_W$ are considerable.

At $\sqrt{s} = M_Z$ both the final state polarization asymmetry for $e^+e^- \to \tau^+\tau^-$ and the initial state left-right asymmetry, for scattering into any final state fermion-antifermion pair, are linearly proportional to $(1-4\sin^2\Theta_W)$. Thus the error in $\sin^2\Theta_W$ obtained from these asymmetries is **independent** of the precise value of the Weinberg angle. A simple calculation shows that, in lowest order,

$$\begin{aligned} A^\tau_{pol}|_{\sqrt{s}=M_Z} &= \frac{\sigma(e^+e^- \to \tau^-_L\tau^+) - \sigma(e^+e^- \to \tau^-_R\tau^+)}{\sigma(e^+e^- \to \tau^-_L\tau^+) + \sigma(e^+e^- \to \tau^-_R\tau^+)}|_{\sqrt{s}-M_Z} \\ &= 2\frac{V_\tau A_\tau}{(V^2_\tau + A^2_\tau)} \simeq 2(1-4\sin^2\Theta_W) \end{aligned} \qquad (III.23)$$

and

$$\begin{aligned} A^f_{LR}|_{\sqrt{s}=M_Z} &= \frac{\sigma(e^+e^-_L \to f\bar{f}) - \sigma(e^+e^-_R \to f\bar{f})}{\sigma(e^+e^-_L \to f\bar{f}) + \sigma(e^+e^-_R \to f\bar{f})}|_{\sqrt{s}=M_Z} \\ &= 2\frac{V_e A_e}{(V^2_e + A^2_e)} \simeq 2(1-4\sin^2\Theta_W) \end{aligned} \qquad (III.24)$$

If one does not have full initial state polarization, and if P_e is the degree of polarization of the initial electron, then what one measures is $P_e A_{LR}$. The linearity of the above formulas

* Recall that at PEP/PETRA A_{FB} was only measured to 2% accuracy.

in $(1 - 4\sin^2\Theta_W)$ implies that, typically, one needs less accurate measurements for these asymmetries to obtain the same error in $\sin^2\Theta_W$ as for A_{FB}. For $\sin^2\Theta_W = 0.23$, Eq (III.21) yields

$$\delta \sin^2\Theta_W \simeq \frac{1}{2}\delta A_{FB} \qquad (III.25)$$

while, from the above, one has

$$\delta \sin^2\Theta_W \simeq \frac{1}{8}\delta A^{\tau}_{pol} = \frac{1}{8}\delta A^{f}_{LR} \qquad (III.26)$$

Furthermore, these latter asymmetries are larger than $A_{FB}\left[A^{\tau}_{pol} \simeq A^{f}_{LR} \simeq 0.16\right]$ and are much less affected by radiative effects [33].

The accuracy that one could actually achieve for $\sin^2\Theta_W$ via a measurement of A_{LR} has been carefully analyzed in a recent report by Treille [34]. He concludes that if 50% longitudinal polarization is achieved, a 40 pb^{-1} exposure at LEP would allow a determination of A_{LR} to $\delta A_{LR} = 0.003$ and consequently one could measure $\sin^2\Theta_W$ to 3-4 parts per 10^4! This is a very much more accurate value for $\sin^2\Theta_W$ than what could be achieved with A_{FB} and it would allow one to test Δr to $\delta\Delta r = 0.001$. However, this measurement will not be done very soon, since even the issue of whether it is feasible to run LEP with polarized beams is still not settled!

In the near term, therefore, the only additional information on $\sin^2\Theta_W$, besides that provided by the forward-backward asymmetry, will come from A^{τ}_{pol}. The way this asymmetry for τ^- leptons can be measured is by looking at the energy distribution of the produced pions, in the decay $\tau^- \to \pi^-\nu_\tau$. In the rest frame of the τ leptons, the decay $\tau^- \to \pi^-\nu_\tau$ is forbidden for $\nu'_\tau s$ produced along the direction of the τ^- polarization, as shown in Fig. III.3.

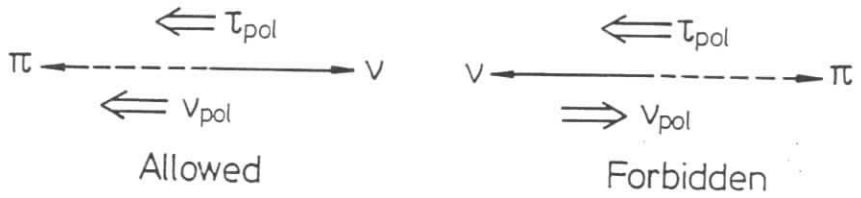

Fig. III.3: Allowed and forbidden configurations in $\tau^- \to \pi^-\nu_\tau$ decays.

If Θ_π is the angle which the pion makes in the τ rest frame, with respect to the τ direction in the laboratory, then it is easy to see that the angular distribution of the produced pions in the τ rest frame is given by

$$\frac{dN}{d\cos\Theta_\pi} \sim (1 - A^{\tau}_{pol}\cos\Theta_\pi) \qquad (III.27)$$

Since the pion energy in the laboratory is related to Θ_π by

$$x_\pi = \frac{E_\pi}{E_{beam}} = \frac{1}{2}(1 + \cos\Theta_\pi) \qquad (III.28)$$

it follows that a measurement of the distribution dN/dx_π will give a direct estimate of A^{τ}_{pol}:

$$\frac{dN}{dx_\pi} \sim [1 - A^{\tau}_{pol}(2x_\pi - 1)] \qquad (III.29)$$

Chaveau [35] estimates that, with a run of 100 days at LEP, one can achieve a statistical accuracy on the τ polarization asymmetry of $(\delta A^{\tau}_{pol})^{stat} \simeq 0.016$, with a systematic error

of half this amount. If this can be achieved, this measurement could provide an extremely accurate value for $\sin^2\Theta_W$. But even if the accuracy were reduced by half, one would still achieve the goal of measuring $\delta\sin^2\Theta_W$ to ± 0.004.

III.2 Neutrino Counting

Soon after their turn-on SLC and LEP, by measuring accurately the total width Γ_{tot} of the Z, should provide us with a very important result concerning the family structure of the standard model. In the $SU(2)\times U(1)$ model, neutrinos of each generation couple universally to the Z boson. If neutrinos beyond ν_e, ν_μ and ν_τ existed, there would be no reason to suppose that they should not also be massless or, at least, very light. Hence, each subsequent generation of neutrinos could give an additional contribution to the total Z width, since the processes $Z \to \nu_i\bar{\nu}_i$ are kinematically allowed. Thus, assuming that there are no other "hidden" modes,

$$\Gamma_{tot} = (\Gamma_{tot})_{3\ gen} + (N_\nu - 3)\Gamma(Z \to \nu\bar{\nu}) \qquad (III.30)$$

Since both $(\Gamma_{tot})_{3\ gen}$ and $\Gamma(Z \to \nu\bar{\nu})$ are well determined theoretically in the standard model, and Γ_{tot} can be well measured at LEP and SLC, these machines should readily ascertain if $N_\nu = 3$ or not. Inferentially, therefore, one can learn in this way if there are more generations of quarks and leptons than the three we already know of.

From the NC interaction Lagrangian of the standard model

$$\mathcal{L}^{NC}_{int} = \frac{e}{\sin\Theta_W\cos\Theta_W} Z^\mu \sum_f \bar{f}[\gamma_\mu V_f + \gamma_\mu\gamma_5 A_f]f \qquad (III.31)$$

it is easy to compute the partial width of the Z into any fermion-antifermion pair. Neglecting m_f relative to M_Z, which is a good approximation for all known fermions except top, one finds

$$\Gamma(Z \to f\bar{f}) = \frac{\alpha M_Z C_f}{3\sin^2\Theta_W\cos^2\Theta_W}[V_f^2 + A_f^2] \qquad (III.32)$$

where C_f is a color factor: $C_f = 1$ for leptons; $C_f = 3$, for quarks.

Several remarks are in order:

i) Eq (III.32) does not include radiative corrections. However, just as we discussed for the case of M_W, the bulk of these effects can be taken into account by replacing α with $\alpha(M_W^2)$ in this equation. Since approximately,

$$\alpha(M_W^2) \simeq \frac{\sqrt{2}}{\pi} G_F M_W^2 \sin^2\Theta_W = \frac{\sqrt{2}}{\pi} G_F M_Z^2 \sin^2\Theta_W \cos^2\Theta_W \qquad (III.33)$$

a more accurate formula for $\Gamma(Z \to f\bar{f})$ is *

$$\Gamma(Z \to f\bar{f}) = \frac{\sqrt{2}}{3\pi} G_F M_Z^3 C_f (V_f^2 + A_f^2) \qquad (III.34)$$

ii) For quarks, in addition to the color factor of 3, one must also take into account QCD effects in which the final state is not just $q\bar{q}$, but also might contain additional gluons. These effects can be easily incorporated to lowest order in α_s by multiplying the rate for quarks by $1 + \frac{\alpha_s(M_Z^2)}{\pi}$. Not surprisingly, this factor is identical to that for the total e^+e^- cross section [37] since, neglecting the quark masses, the QCD corrections to the vector and axial vertex are the same. Hence, for quarks, really

$$C_q \to 3[1 + \frac{\alpha_s(M_Z^2)}{\pi} + ...] \simeq 3[1.04 \pm 0.01] \qquad (III.35)$$

where we have used a recent estimate [38] for the running coupling constant $\alpha_s(M_Z^2)$.

iii) Given the recent $UA1$ bound on m_t [28], $m_t \geq 44 - 56$ GeV, it is unlikely that kinematically the process $Z \to t\bar{t}$ is allowed. In what follows we shall, therefore, neglect it altogether. However, when LEP and SLC are running one can rather readily determine experimentally whether $Z \to t\bar{t}$ is allowed or not, since the process $Z \to t\bar{t}$ leads to multijet events $t \to b \to c$ which are easily identifiable.

* Typically, the residual electroweak corrections to (III.34) are only about 1-2 per mil of $\Gamma(Z \to f\bar{f})$ [36].

Using Eq (I.12) and choosing, for definitiveness, as parameters $\sin^2\Theta_W = 0.23$ and $M_Z = 92$ GeV, one finds for the partial widths of the Z to go into the different types of quarks and leptons the following results

$$\begin{aligned} \Gamma(Z \to \nu\bar{\nu}) &= 170 MeV \\ \Gamma(Z \to e^+e^-) &= 86 MeV \\ \Gamma(Z \to u\bar{u}) &= 306 MeV \\ \Gamma(Z \to d\bar{d}) &= 393 MeV \end{aligned} \qquad (III.36)$$

Hence, neglecting the top contribution, one has for the total width

$$(\Gamma_{tot})_{3\ gen} = 2560\ MeV \qquad (III.37)$$

The above result has two kinds of uncertainties. There is a trivial uncertainty in the actual numerical value in (III.37) connected with the fact that we do not know yet the best central values for M_Z and $\sin^2\Theta_W$. When these parameters are measured accurately at SLC and LEP the actual number for $(\Gamma_{tot})_{3\ gen}$ may be different than 2560 MeV. But this is irrelevant, since given some new values for M_Z and $\sin^2\Theta_W$, one can always compute $(\Gamma_{tot})_{3\ gen}$ anew. There remains, however, some intrinsic uncertainty in $(\Gamma_{tot})_{3\ gen}$ due to the experimental errors on $M_Z, \sin^2\Theta_W$ and $\alpha_s(M_Z^2)$. This intrinsic uncertainty is very small and one find

$$\delta(\Gamma_{tot})_{3\ gen} = (\pm 4 \pm 10 \pm 20)\ MeV \qquad (III.38)$$

with the errors above coming, respectively, from $\delta M_Z = \pm 50 MeV$, $\delta \sin^2\Theta_W = \pm 0.004$ and $\delta\left(\frac{\alpha_s}{\pi}\right) = \pm 0.01$. The intrinsic errors in Eq (III.38) are all much less than the additional width $\Gamma(Z \to \nu\bar{\nu}) \simeq 170\ MeV$ which would arise from one extra neutrino species. Thus, provided one can measure Γ_{tot} with good accuracy, Eq (III.30) should easily allow one to distinguish between having 3 or 4 neutrino species.

At LEP and SLC the total Z width can be measured rather well by studying the process $e^+e^- \to \mu^+\mu^-$. However, this analysis is not trival in that radiative effects substantially alter the naive expectations. Only after these radiative effects are accounted for, can one hope to extract a Z width suitable for comparsion with the theoretical formulas discussed

above. Let me elaborate on this point a bit. The total cross section for the $e^+e^- \to \mu^+\mu^-$ process, to lowest order in α, follows by integrating Eq. (III.12) over θ:

$$\sigma(s) = \frac{4\pi\alpha^2}{3s} F_1(s) \qquad (III.39)$$

Near $\sqrt{s} = M_Z$ the last term in $F_1(s)$ in Eq (III.13a), coming from pure Z exchange, dominates and $\sigma(s)$ takes a Breit-Wigner form. Using Eq (III.32), one can write (III.39), as

$$\sigma(s)|_{\sqrt{s}\simeq M_Z} \simeq 12\pi \frac{\Gamma(Z \to e^+e^-)\Gamma(Z \to \mu^+\mu^-)}{(s - M_Z^2)^2 + M_Z^2\Gamma_{tot}^2} \qquad (II.40)$$

This expression is symmetric about $\sqrt{s} = M_Z$ and one naively would imagine that a measurement of this line shape would yield Γ_{tot}.

This naive expectation, however, is not fullfilled in practice, since QED radiative effects substantially alter the line shape. The principal modifications arise because of initial state radiation from the incident e^+ and e^- beams (see Fig. III.4).

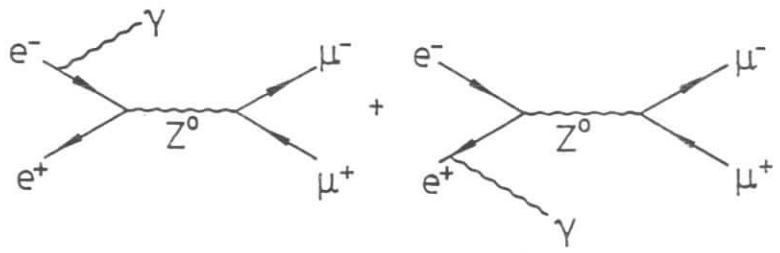

Fig. III.4: Initial state radiation, giving rise to line shape modifications.

Kinematically the effect of this initial state radiations is to:

i) shift the peak for the process $e^+e^- \to \mu^+\mu^-$ above $\sqrt{s} = M_Z$.

ii) give rise to a long radiative tail for $\sqrt{s} > M_Z$.

Both these phenomena are illustrated in Fig. III.5, where the lowest order cross section is contrasted with what is expected once one includes first order QED corrections, for a reasonable set of experimental cuts.

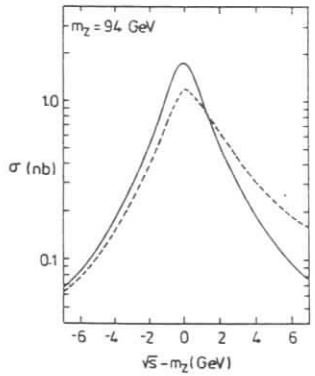

Fig. III.5: Total cross section for the process $e^+e^- \to \mu^+\mu^-(\gamma)$ in lowest order (solid line) and QED corrected (dashed line), from [39]. The parameters and cuts used here are: $M_Z = 94\ GeV$, $\Gamma_Z = 2.67\ GeV$, $\sin^2\Theta_W = 0.2157$ and $E_{\mu^+}, E_{\mu^-} > 10\ GeV$, $5^0 \leq \Theta_{\mu e} \leq 175^0$, $\xi_{acol} = 10^0$.

The size of these effects can be estimated roughly to give a mass shift δM_Z and an increase in the width $\delta\Gamma_Z$ of order [40].

$$\delta M_Z^{em} \sim \delta\Gamma_Z^{em} \sim \frac{\alpha}{\pi}\ell n\frac{M_Z^2}{m_e^2}\Gamma_{tot} \sim 150 MeV \qquad (III.41)$$

Thus these effects are far from negligible and one needs to unfold them to extract accurate values for Γ_{tot} and M_Z.

Using the QED corrected line shape, however, it is expected that the actual experimental error incurred for Γ_{tot} will be much smaller than $\delta\Gamma_Z^{em}$. This issue has been studied by Blondel et al for LEP [41]. They suggested performing a scan from $\sqrt{s} = 80\ GeV$ to $\sqrt{s} = 104\ GeV$ with a 2 GeV step interval. Assuming that one can collect $2pb^{-1}$ integrated luminosity per point, one would have approximately 4500 $\mu^+\mu^-$ pairs, of which 2000 in the peak, after the scan. This procedure, which should take from one to three months running time at LEP, should give a statistical error on Γ_{tot} of [41]

$$\delta\Gamma_{tot}^{stat} \leq 15\ MeV \qquad (III.42)$$

Blondel et al [41] also estimate that possible quadratic distorsions in the machine luminosity versus energy - distorsions which would lead to a change in the $e^+e^- \to \mu^+\mu^-$ profile - could give rise to a systematic uncertainty of order

$$\delta\Gamma \leq 10\ MeV \qquad (III.43)$$

If indeed one can keep the errors in Γ_{tot} at LEP and SLC to the levels indicated in Eqs (III.42) and (III.43), it should be very straight forward to do neutrino counting to better than one generation. At present, we already have some information on N_ν, but all of it involves either some further assumptions or it is not that restrictive. The present best bounds on N_ν are summarized in Table III.1 [42]

Table III.1 Bounds on N_ν

Bound	Source
$N_\nu \leq 4$	Primordial Nucleosynthesis
$N_\nu \leq 5$	$\sigma_Z B(Z \to e^+e^-)/\sigma_W B(W \to e\nu_e);\ m_t \leq 50 GeV$
$N_\nu \leq 3$	$\sigma_Z B(Z \to e^+e^-)/\sigma_W B(W \to e\nu_e);\ m_t \geq 70 GeV$
$N_\nu \leq 4.6$	$e^+e^- \to \gamma\ nothing$

The bound on N_ν from the process $e^+e^- \to \gamma\ nothing$ indicated in Table III.1 was obtained at PEP and PETRA. This same reaction can be studies at LEP and SLC and provides a

more "direct" method for counting neutrinos than just measuring the Z width does. I want to close this subsection by making some remarks on this alternative method of neutrino counting.

In the process $e^+e^- \to \gamma$ *nothing*, the "nothing" stands for any kind of neutral penetrating particle and it includes, in particular, neutrino pairs. Near the Z resonance, this latter process gets dominant contributions from the presence of the virtual Z propagator. The relevant diagrams are illustrated in Fig. III.6.*

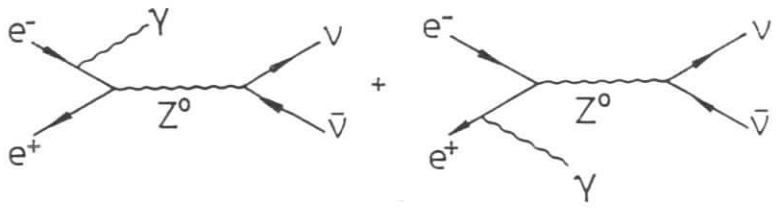

Fig. III.6: Graphs contributing to the process $e^+e^- \to \gamma\nu_i\bar{\nu}_i$

The size of the cross section depends directly on the partial width of the Z into all the unseen neutral excitations. Thus a measurement of $e^+e^- \to \gamma$ *nothing* serves directly as a neutrino counter [43].

The cross section for the process $e^+e^- \to \gamma$ *nothing*, computed some time ago by Gaemers, Gastmans and Renard [43] reads

$$\frac{d\sigma}{dxdy} = \frac{\alpha G_F^2 s(1-x)}{3\pi^2 x(1-y^2)}\Big[\ (1-\frac{1}{2}x)^2 + \frac{1}{4}x^2y^2\ \Big]F(x) \qquad (III.44)$$

* For the process $e^+e^- \to \gamma\nu_e\bar{\nu}_e$ there are additional CC graphs, besides those shown in Fig. III.6.

where

$$F(x) = 1 + \frac{2M_Z^2(M_Z^2 - s(1-x))(V_e - A_e) + 2M_Z^4 N_\nu(V_e^2 + A_e^2)}{[M_Z^2 - s(1-x)]^2 + M_Z^2\Gamma_{tot}^2} \qquad (III.45)$$

In the above the parameters x and y are related to the photon energy and its angle, θ_γ, relative to the incoming e^- direction

$$x = \frac{2E_\gamma}{\sqrt{s}};\quad y = \cos\theta_\gamma, \qquad (III.46)$$

while N_ν is the total number of neutrino species.

Two points are worth remarking upon regarding this expression:

i) The numerator factor in $F(x)$ is not purely proportional to N_ν because of the interference between the CC and NC contributions in the process $e^+e^- \to \nu_e\bar{\nu}_e\gamma$

ii) For energies close to the Z mass, however, the terms involving the Z propagator - and therefore involving the number of neutrinos - are very much enhanced in $F(x)$. This enhancement peaks at $x = 1 - \frac{M_Z^2}{s}$, which corresponds to (for $\sqrt{s} \simeq M_Z$):

$$E_\gamma = \frac{\sqrt{s}}{2}(1 - \frac{M_Z^2}{s}) \simeq \sqrt{s} - M_Z \qquad (III.47)$$

The differential cross section for the process $e^+e^- \to \gamma$ *nothing*, for the case in which *nothing* is just the contribution of the neutrinos of 3 generations (therefore $N_\nu = 3$) is plotted in Fig. III.7. In this figure, the dependence on $\cos\theta_\gamma$ has been integrated over, for photon angles lying in the interval $20^0 < \theta_\gamma < 160^0$. This angular cut, as I will discuss below, is done to suppress background. One sees that, as one increases the center of mass energy $\sqrt{s}$, the peak in the photon spectrum shifts, as predicted by Eq (III.47). The height

of the peak is proportional to N_ν, which for this figure is taken as 3. Note also that the cross section decreases as E_γ increases, due to the $1/x$ factor in Eq (III.44).

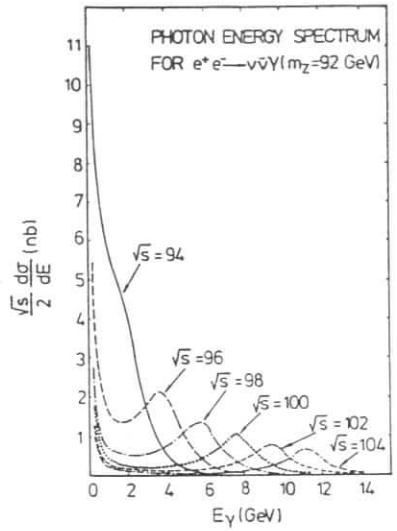

Fig. III.7: Cross section for $e^+e^- \to \gamma$ *nothing* for $N_\nu = 3$, integrated over all photon angles in the range $20^0 < \theta_\gamma < 160^0$, from [44]

Whether one can count the number of neutrinos this way at LEP and SLC depends mostly on how successful one is in suppressing the normal QED background from the process $e^+e^- \to e^+e^-\gamma$, in which both final charged particles are lost in the beam pipe. Since photons produced at large θ_γ with respect to the beam axis, in general, do not arise from configurations with forward going electrons or positrons, the cut shown in Fig. III.7 should substantially reduce background. However, as Caffo, Gatto and Remiddi [45] point out, this may not be enough. These authors, in their analysis, find a much larger background than previously estimated, especially for relatively low photon energies. This is illustrated, for instance, in Fig. III.8 where the signal expected for $N_\nu = 3$, for a cut of $25^0 < \Theta_\gamma < 155^0$, is compared to the background calculation of Caffo, Gatto and Remiddi [45], for a center of mass energy of 5 GeV above the Z mass.

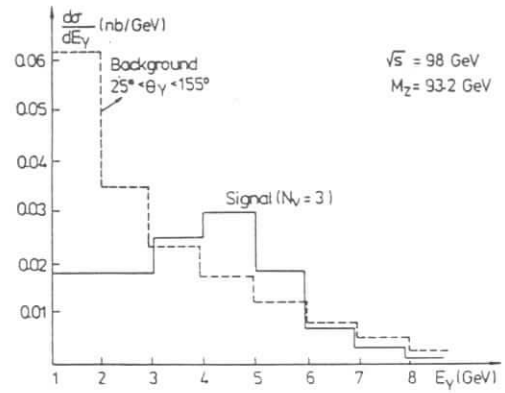

Fig. III.8: Signal and background for a neutrino counting experiment with $25^0 < \theta_\gamma < 155^0$ and $\sqrt{s} - M_Z \simeq 5GeV$, from [45].

An independent calculation by Maña and Martinez [46] which treated a sensitive numerical integration region in a different way than was done in [45], appears to give very similar results.

In view of the rather large background found, Caffo, Gatto and Remiddi [45] suggest that it may be sensible to try to do the neutrino counting experiment at energies only slightly above the Z mass. Here the cross section, as can be seen from Fig. III.7, is rather large and, if an accurate background subtraction can be performed, one may in the end be better off. This same point was made sometime ago also by Bartels, Fridman, Wu and Schwartz [47]. An alternative possibility, however, is to run at energies much above the Z mass where, even though the cross section is smaller, the background is really rather negligible. Forthcoming experiments at LEP and SLC will have to decide which is the best strategy to pursue, in this alternative method of neutrino counting.

III.3 Testing the Three Gauge Couplings

Radiative effects are an indirect way to test the non Abelian couplings in the standard

$SU(2) \times U(1)$ model. However, since these are virtual effects even if a discrepancy were to be found, it would not be obvious to what to ascribe it to. Fortunately, with LEP 200 (LEP operated at a CM energy of $\sqrt{s} \simeq 200\ GeV$) one will be able to study directly the three gauge vertex, by looking for direct production of W^+W^- pairs. This will afford the first opportunity to actually see the non Abelian nature of the $SU(2) \times U(1)$ model at work.

The process $e^+e^- \to W^+W^-$ is interesting for many different reasons and its study will constitute the mainstay of the experimental program for LEP 200. As Fig. III.9 indicates, for instance, all three interactions in the standard model: CC, NC and *em* are directly involved in the $e^+e^- \to W^+W^-$ process.

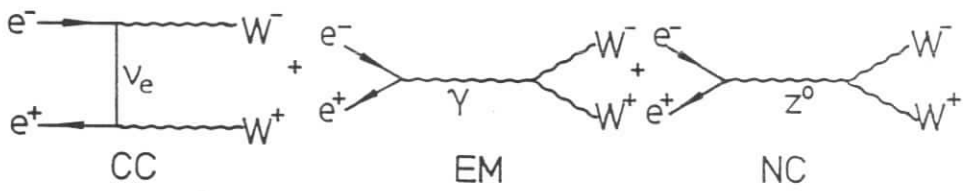

Fig. III.9: Lowest order contributions to the process $e^+e^- \to W^+W^-$

Furthermore, the graphs in Fig. III.9 due to γ and Z exchange involve the three gauge vertex $\Gamma_V^{\mu\alpha\beta}$, with $V = \gamma$ or $V = Z$. As we indicated in Sec I [c.f. Fig. I.1], these vertices are related, since they both stem from the nonvanishing non Abelian $SU(2)$ coupling $W_3W^+W^-$. From Eqs (I.18) and (I.19) one readily deduces that, in momentum space,

$$\Gamma_V^{\mu\alpha\beta}(p,q,\bar{q}) = ig_V\{(\bar{q}-q)^\mu \eta^{\alpha\beta} + (p-\bar{q})^\alpha \eta^{\mu\beta} + (q-p)^\beta \eta^{\mu\alpha}\} \qquad (III.48)$$

Here $\eta^{\alpha\beta}$ is the metric tensor and the relevant kinematical notation is indicated in Fig. III.10. The coupling constants g_V for the γ and the Z are

$$g_Z = g\cos\Theta_W = e\ cot\Theta_W;\quad g_\gamma = g\sin\Theta_W = e \qquad (III.49)$$

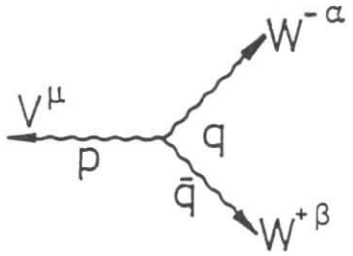

Fig. III.10: The three gauge vertex in momentum space. Note that $p + q + \bar{q} = 0$.

It is straight forward to calculate the cross section for the process $e^+e^- \to W^+W^-$, using the Feynman diagrams of Fig. III.9. This computation was done first in the middle 1970's by Shuskov, Flambaum and Khriplovich [48] and by Alles, Boyer and Buras [49]. The result for the total cross section can be written in the following convenient way, by using the shorthands $\beta = \sqrt{1-4\lambda}$ and $\lambda = \frac{M_W^2}{s}$:

$$\begin{aligned}\sigma(e^+e^- \to W^+W^-) = &\frac{\pi\alpha^2\beta}{2s\sin^4\Theta_W}\Big\{\Big[(1+2\lambda+2\lambda^2)\frac{1}{\beta}ln\ \Big(\frac{1+\beta}{1-\beta}\Big) - \frac{5}{4}\Big] \\ &+ \frac{M_Z^2(1-2\sin^2\Theta_W)}{(s-M_Z^2)}\ \Big[\ 2(2\lambda+\lambda^2)\frac{1}{\beta}ln\ \Big(\frac{1+\beta}{1-\beta}\Big) - \frac{1}{12\lambda} - \frac{5}{3} - \lambda\ \Big] \\ &+ \frac{M_Z^4(8\sin^4\Theta_W - 4\sin^2\Theta_W + 1)}{48(s-M_Z^2)^2}\Big[\beta^2\Big(\frac{1}{\lambda^2} + \frac{20}{\lambda} + 12\Big)\Big]\Big\}\end{aligned} \qquad (III.50)$$

One can immediately deduce from the above several important features:

i) Near threshold ($\beta \to 0;\ \lambda \to \frac{1}{4}$), only the first square bracket survives and one finds

$$\sigma_{thresh} \simeq \Big[\frac{\pi\alpha^2}{4\sin^4\Theta_W M_W^2}\Big]\beta \simeq [46\ pb]\beta \qquad (III.51)$$

Since the peak of the cross section given in (III.50) is only about 20 pb, one sees that already 500 MeV above threshold ($\beta \simeq 0.1$) the W^+W^- cross section is sizable, being near 5 pb. Of course, with such a fast rise, it is incorrect to neglect the finite width of the W here, since this width is several GeV wide. Nevertheless, all the width will do is to smooth out this rise by giving a tail of events already before the nominal threshold at $\sqrt{s} = 2M_W$.

ii) In the opposite limit, at high energy ($\beta \to 1$; $\lambda \to 0$) again the first square bracket in (III.50) dominates and one deduces that

$$\sigma \underset{s >> M_W^2}{\to} \left[\frac{\pi\alpha^2}{2\sin^4\Theta_W}\right]\frac{1}{s}\ell n\frac{s}{M_W^2} \qquad (III.52)$$

So this cross section decreases only logarithmically less rapidly than the annihilation cross section for fermion-antifermion production [e.g. Eq (III.39)]

The behavior of the total cross section for $e^+e^- \to W^+W^-$ in the range of interest for LEP 200 is shown in Fig. III.11, both including and excluding the contribution of the width of the W bosons. One sees that after the rapid threshold growth, the cross section flattens out around $E_{beam} \simeq 100\ GeV$ ($\sigma_{max} \simeq 17\ pb$) and then slowly decreases.

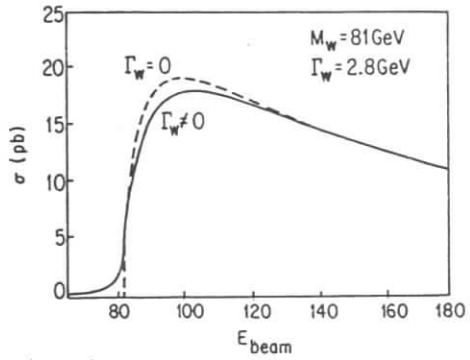

Fig III.11: Total cross section for the process $e^+e^- \to W^+W^-$ in the standard model.

The presence of the three gauge vertex is crucial to obtain the good asymptotic behavior displayed in Fig. III.11 and apparent in Eq (III.52) [50]. In fact, if one computes the cross section for W^+W^- production retaining only the neutrino exchange contribution in Fig. III.9, the resulting expression grows with energy and, eventually, violates unitarity:

$$\sigma_{\nu\ exch} \underset{s >> M_W^2}{\to} \left[\frac{\pi}{48}G_F^2\right]s \qquad (III.53)$$

The contrast between the standard model prediction for $\sigma(e^+e^- \to W^+W^-)$ and the cross section obtained by keeping only the neutrino exchange graph is shown in Fig. III.12. One sees that, unfortunately, the effect of the cancellation resulting from the presence of three gauge vertex is not so apparent at LEP 200 energies. Indeed, in this energy region, to study the three gauge vertex it is much more sensible to look at a less integrated quantity than the total cross section [51]; for example, the W angular distribution.

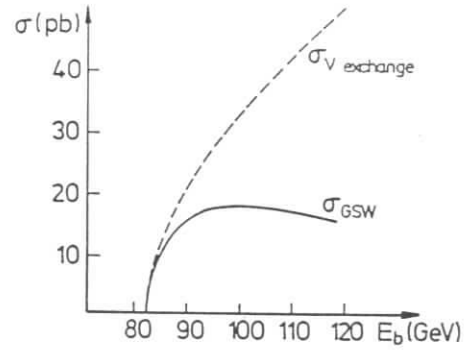

Fig. III.12: Comparison of the neutrino exchange cross section to that of the standard model for the process $e^+e^- \to W^+W^-$.

The angular distribution of the produced W bosons is influenced markedly by the ν exchange graph in Fig. III.9. This graph contains a t- channel pole because of the zero mass of the neutrinos, and this factor favors the production of the W^- bosons along the direction of the incoming e^-. This forward peaking increases with increasing beam energy,

as can be seen in Fig. III.13.

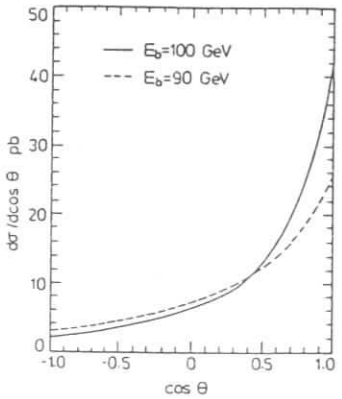

Fig. III.13: W^- angular distribution for two beam energies. Here θ is the angle the W^- makes with respect to the incident e^- direction.

By carefully studying this angular distribution at LEP 200, one can probe the structure of the three gauge vertex. For instance, if the W boson were to have an anomalous magnetic moment κ, * giving a W magnetic moment [52]

$$\mu_W = \frac{e}{2M_W}[1+\kappa], \qquad (III.54)$$

then the coefficient for the last two terms in (III.48) would be multiplied by $\frac{1}{2}[1+\kappa]$. LEP 200 can look for the presence of such a term. Qualitatively [51], if $\kappa > 1$ the forward peaking in Fig. III.13 increases, while for $\kappa < 1$ in contrast one has a larger backward tail. Both of these effects become more pronounced as the energy increases. It has been estimated by Barbiellini et al [51] that with an exposure at LEP 200 of 500 pb^{-1} - corresponding to one year of running at design luminosity - one could determine a 10% departure of κ from unity, while a 50 pb^{-1} run could check κ to the 50% level.

A second interesting study that can be performed at LEP 200 concerns the helicity states of the produced $W's$. By angular momentum conservation, it is easy to convince oneself that

* κ contributes also to the W electric quadrupole moment: $Q_W = -\frac{e\kappa}{M_W^2}$

precisely in the forward direction one of the produced $W's$ must be longitudially polarized. The graphs of Fig. III.9 all involve vectorial vertices, so that, neglecting electron mass effects, the process $e^+e^- \to W^+W^-$ can only occur if the incident electrons and positrons have opposite helicity. Hence, as shown in Fig. III.14, in the forward direction the final W helicity must also be ± 1. Because of the presence of the neutrino exchange graph, it turns out that $\sigma_{LR} >> \sigma_{RL}$. Thus one expects the dominant helicity configuration for forward going $W's$ to be either a W^- with $\lambda = -1$ and a W^+ with $\bar{\lambda} = 0$, or a W^- with $\lambda = 0$ and a W^+ with $\bar{\lambda} = +1$.

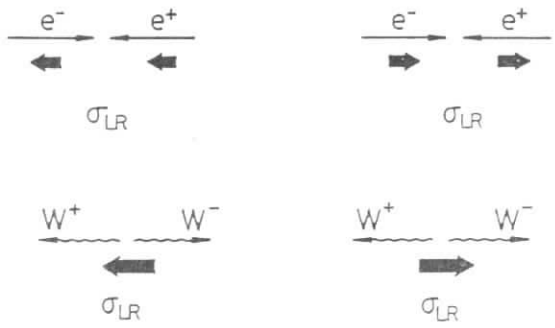

Fig. III.14: Helicity configurations in $e^+e^- \to W^+W^-$ scattering in the forward direction.

The presence of longitudinally polarized $W's$ in the final state is very interesting, since the presence of this polarization state is directly connected to the existence of a W mass and hence to the breakdown of $SU(2) \times U(1)$. Unfortunately, except near the forward direction transverse W production dominates. Hagiwara et al [53] have studied in detail the fraction of $W's$ produced at LEP 200 with a given polarization and a given production angle. Their results, which update and complement an earlier study by Gaemers and Gounaris [54] are displayed in Fig. III.15

One notes from this figure that:

i) Apart from $\theta \approx 0$, where $W^-(-1)W^+(0)$ or $W^-(0)W^+(1)$ must dominate, by angular momentum conservation, the main polarization states produced are $W^-(-1)W^+(+1)$.

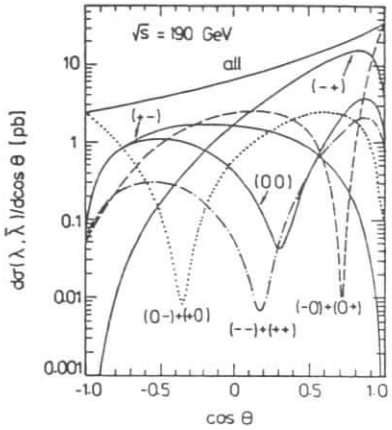

Fig. III.15: Angular distribution for the process $e^+e^- \rightarrow W^+W^-$ at $\sqrt{s} = 190\ GeV$ for different polarizations $(\lambda, \bar{\lambda})$ of the produced W^- and W^+ bosons, from [53].

ii) The interesting $W_{long}\ W_{long}$ configuration (0,0) is not very relevant, except close to the forward direction. But even there it is a factor of five smaller than the transverse-transverse and transverse-longitudinal cross section.

In principle, one can try to separate out the various polarization contributions experimentally, by using the angular distribution of the produced fermions as a polarization analyzer. To do this, it is necessary to determine the direction of the W axis in the event. This is facilitated because, kinematically, the energy of the produced W must be that of the beam energy. Once this axis is determined, one can boost back the event to the W rest frame. In this frame, the angular distribution of the produced fermions (which materialize experimentally as jets if the fermions are quarks), depends on the W helicity. Let Θ^* be the angle of a produced e^- (or d quark) with respect to the W^- axis in the W rest frame. Then, because of the (V - A) form of the charged weak interactions, one finds the following angular distributions:

$$\frac{dN}{d\cos\Theta^*} \sim \begin{cases} \frac{1}{2}(1+\cos\Theta^*)^2 & \lambda = -1 \\ \sin^2\Theta^* & \lambda = 0 \\ \frac{1}{2}(1-\cos\Theta^*)^2 & \lambda = +1 \end{cases} \qquad (III.55)$$

There are many other detailed investigations possible at LEP 200 [55]. Perhaps one of the most interesting one concerns trying to get an accurate measurement of the W mass itself. Four methods have been suggested for doing this [51]:

i) Obtain M_W by studying the threshold dependence of the total W^+W^- cross section.

ii) Extract M_W from the end point spectrum in $W \rightarrow e\nu_e$.

iii) Reconstruct M_W from the jet-jet invariant mass from the decays $W \rightarrow 2jets$.

iv) Reconstruct M_W from the ν_e invariant mass in the decays $W \rightarrow e\nu_e$.

A careful study of these different techniques has been carried out by Roudeau et al [56]. They conclude that by using a combination of the above methods one should be able to attain a precision for M_W of order $\delta M_W \leq 100\ MeV$. Obviously, if this can be done, this measurement would allow a further test of radiative corrections. Independently, of a separate measurement of $\sin^2\Theta_W$, the radiative shift Δr can directly be probed experimentally once one knows M_Z and M_W accurately [cf Eq (III.1)].

I end this subsection with just a short remark on the last method above. At first sight it is somewhat puzzling how one could reconstruct the W mass from the $\nu_e e$ invariant mass, given that the neutrinos leave the apparatus! The trick here is that at LEP 200, for the process $e^+e^- \rightarrow W^+W^-$, the W energy is just the beam energy, E_b. It is then easy to convince onself that the kinematics is totally determined once the W axis is fixed and the electron energy and scattering angle are measured. Consider for example the 2 jet $e\nu_e$ decay shown schematically in Fig. III.16. The W mass is given by

$$M_W^2 = 2E_eE_\nu(1-\cos\Theta_{e\nu}) \qquad (III.56)$$

Once E_e is measured E_ν follows from energy momentum conservation: $E_\nu = E_b - E_e$. Furthermore, the angle $\Theta_{e\nu}$ between the electron and the neutrino is fixed from a measurement of Θ_W and Θ_e, since the neutrino momentum transverse to the W direction must

balance that of the electron direction.

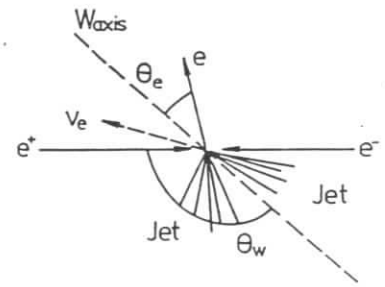

Fig. III.16: The process $e^+e^- \to W^+W^- \to 2jet\ e\nu_e$

III.4 Looking for Higgs

Probably one of the most important open issues in the standard model is the question if there is, or if there is not, an elementary Higgs boson, as predicted by the simplest method to break $SU(2)\times U(1)$ down. Recall from Eq (I.30) that the Higgs boson mass M_H was not fixed, since it depended on the unknown parameter λ detailing the strength of the Higgs self interactions, in the symmetry breaking potential. There are a number of arguments in the literature, of differing degrees of rigor, which give an upper bound on M_H. * Very crudely speaking, these arguments all use the fact that if λ is too big, or equivalently if $M_H >> v$ - the natural scale of the weak interations - some inconsistences arise in the theory.

Perhaps the most rigorous of the bounds on M_H comes from the work of Luescher and Weisz [57]. One can qualitatively understand their considerations by looking at the running

* There are also a, somewhat weaker, variety of considerations which provide a lower bound for the Higgs mass.

coupling $\lambda(q^2)$. Effectively, the Higgs mass is fixed by the formula

$$M_H^2 = 2\lambda(M_H^2)v^2 \qquad (III.57)$$

Because $\lambda(q^2)$ is not asymptotically free, as q^2 increases, $\lambda(q^2) \to \infty$. So one must really view the Higgs sector as an effective field theory with some cutoff. However, if $\lambda(M_H^2)$ is sufficently large, one finds that this cutoff Λ gets to be **smaller** than M_H itself! Hence, $\lambda(M_H^2)$ and M_H must both be bound. The bound found in this way is [57]

$$M_H \leq 630\ GeV \qquad (III.58)$$

This analytical result has been confirmed recently by a Monte Carlo analysis [58]

More than ten years ago, Lee, Quigg, and Thacker [59] obtained a similar bound, by observing that tree level unitarity is violated if M_H is too big. Because the longitudinal pieces of the weak bosons are sensitive to the symmetry breaking sector, it is sensible to concentrate specifically on the scattering of these longitudinal gauge bosons. If one writes for the amplitude for W_LW_L scattering, T_{LL}, a partial wave expansion

$$T_{LL}(s,t) = 16\pi \sum_J (2J+1) a_{LL}^J(s) P_J(\cos\theta), \qquad (III.59)$$

then calculating the tree level diagrams for the scattering, one finds for the partial waves

$$a_{LL}^J(s) = A^J(\frac{s}{M_W})^2 + B^J(\frac{s}{M_W}) + C^J \qquad (III.60)$$

The first two terms above, if present, would violate unitarity. However, one can easily check by direct calculation that both A^J and B^J cancel in the standard model [59]. This cancellation is analogous to the gauge cancellation we observed earlier for the process $e^+e^- \to W^+W^-$. The coefficient C^J does not, per se, violate unitarity, provided it is not

too big. It turns out, however, that for $J = 0, a^0_{LL}$ is directly proportional to M_H, which allows one then to set a bound on M_H. One finds, in the limit $\sqrt{s} >> M_H$, that [59]

$$a^0_{LL} = -\frac{G_F M_H^2}{4\pi\sqrt{2}} \qquad (III.60)$$

Since unitarity requires that

$$| a^0_{LL} | \leq 1 \qquad (III.61)$$

this constrains M_H to be less or equal to about one TeV [59]:

$$M_H^2 << \frac{4\pi\sqrt{2}}{G_F} \sim 0(TeV^2) \qquad (III.62)$$

One can arrive at the above bound in another manner. Using Eq (I.29) one can compute the width of the Higgs boson to decay into W's and Z's as:

$$\Gamma(H \to W^+W^-) = \frac{G_F M_H^3}{8\pi\sqrt{2}}\left[1 - 4\frac{M_W^2}{M_H^2} + 12\frac{M_W^4}{M_H^4}\right]\left[1 - 4\frac{M_W^2}{M_H^2}\right]^{\frac{1}{2}} \qquad (III.63a)$$

$$\Gamma(H \to ZZ) = \frac{G_F M_H^3}{16\pi\sqrt{2}}\left[1 - 4\frac{M_Z^2}{M_H^2} + 12\frac{M_Z^4}{M_H^4}\right]\left[1 - 4\frac{M_Z^2}{M_H^2}\right]^{\frac{1}{2}} \qquad (III.63b)$$

One sees that the above partial widths grow like M_H^3. Hence, for M_H large, they will eventually be much larger than the Higgs mass itself and one will cease to believe this perturbative answer. Asking that the total Higgs width $\Gamma_{tot} \leq M_H$, gives a similar bound to (III.62). This should not be surprising, since this result is not unrelated to what we did earlier. The cubic growth of Γ with M_H comes, in fact, from decays of the Higgs boson into W_L or Z_L pairs. The decay amplitude into these helicity figurations is proportional to the polarization vector for longitudinal helicity states:

$$A(H \to W_L W_L) \sim \epsilon_L(p_1) \cdot \epsilon_L(p_2) \qquad (III.64)$$

Thus, since $\epsilon^\mu_L(p) \sim \frac{p^\mu}{M_W}$, A is proportional to $\frac{M_H^2}{M_W^2}$.

The above bounds are interesting, but not too encouraging for experiment. In the near future the big new e^+e^- machines LEP and SLC, operating at the Z, will only be able to carry through Higgs searches for $M_H \leq 40 - 50\ GeV$. LEP 200 may get to nearly double this range, but one will have to wait for the SSC to try to push the exploration limits for the Higgs near to the above theoretical bounds. Even so, there will always be a region between $M_H \simeq 80\ GeV$ (which one can probe with LEP 200) and $M_H \simeq 2M_W$ where it will be very difficult to access the Higgs experimentally [60].

If $M_H < 2M_W$, the Higgs will decay into the heaviest pair of fermions since, according to Eq (I.36), its coupling is proportional to m_f. One finds, by a straight forward calculation,

$$\Gamma(H \to f\bar{f}) = \frac{G_F m_f^2}{4\sqrt{2}\pi} M_H C_f \left[1 - 4\frac{m_f^2}{M_H^2}\right]^{\frac{3}{2}} \qquad (III.65)$$

This is a very narrow width. For instance, for $M_H = 60\ GeV$, since $m_t > 30\ GeV$, the dominant mode of decay is $H \to b\bar{b}$ which, using the above formula, gives $\Gamma(H \to b\bar{b}) \simeq 3\ MeV$!. Although the $b\bar{b}$ channel dominates in this case the rate into $\tau^+\tau^-$ pairs is not totally negligible

$$\frac{\Gamma(H \to \tau^+\tau^-)}{\Gamma(H \to b\bar{b})} \simeq \frac{1}{3}\left(\frac{m_\tau}{m_b}\right)^2 \simeq 0.03 \qquad (III.66)$$

If the Higgs mass is less than about 50 GeV its discovery at LEP and SLC should be possible through the Bjorken process [61] $e^+e^- \to H\ell^+\ell^-$, or its companion $e^+e^- \to H\nu\bar{\nu}$ (See Fig. III.17). The latter process has a larger cross section, but it also has a bigger background. A direct calculation of the differential decay width for the dilepton process, using the HZZ vertex of Eq (I.29), gives the expression [61]

$$\frac{d\Gamma(Z^0 \to H\ell\bar{\ell})}{dx} = \frac{\alpha}{\pi \sin^2 2\Theta_W} \frac{[1 - x + \frac{x^2}{12} + \frac{2z^2}{3}][x^2 - 4z^2]^{\frac{1}{2}}}{[x - z^2]^2} \qquad (III.67)$$

Here $x = 2E_H/M_Z$ and $z = M_H/M_Z$, with the kinematic range for x being given by

$$2z \leq x \leq 1 + z^2 \qquad (III.68)$$

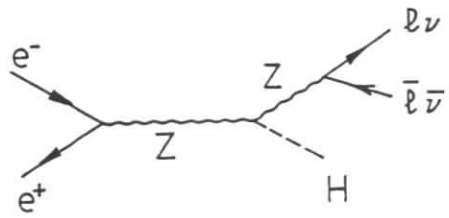

Fig. III.17: Diagram contributing to $H\ell^+\ell^-$ or $H\nu\bar{\nu}$ production at the Z pole.

Because of the Z propagator factor, the differential rate (III.77) favors the production of lepton pairs with as large an invariant mass as possible. One has

$$m_{\ell\bar{\ell}} = M_Z(1 + z^2 - x)^{1/2} \rightarrow M_Z - M_H \qquad (III.69)$$

This peaking behaviour, which constitutes a characteristic signature for the decay $Z \rightarrow H\ell\bar{\ell}$, is a useful handle to have, since the total branching ratio for this process drops rather rapidly as a function of the Higgs mass, as illustrated in Fig. III.18. Note that for $M_H \sim 40\ GeV$, one is left with just a handful of events of the type $H\ell^+\ell^-$ for every million $Z's$. Thus it is very important that the signature be distinctive, if one is to have any hope to dig out such a rare signal. Indeed, careful studies [62] indicate that one should be able to detect in this way a Higgs boson, if $M_H \leq 50\ GeV$.

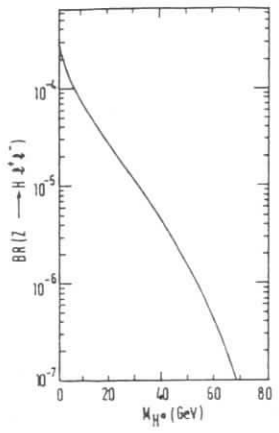

Fig. III.18: Branching ratio for the process $Z \rightarrow H\ell^+\ell^-$ as a function of the Higgs mass, from [62]

It could well be, however, that the Higgs mass is above 50 GeV. In that case, LEP 200 would then have some possibility of detecting the Higgs via its associated production with a real Z boson. The relevant diagram is the same as that in Fig. III.17, except that now the produced Z is real and not virtual. The cross section for the process $e^+e^- \rightarrow ZH$ has been calculated by a number of authors [63], with a particularly complete set of formulas being given by Kelly and Shimada, who also considered the subsequent decay of the Z into lepton pairs. One finds

$$\sigma(e^+e^- \rightarrow ZH) = \frac{\pi\alpha^2[1 + (1 - 4\sin^2\Theta_W)^2]P(P^2 + 3M_Z^2)}{24\sin^4\Theta_W\cos^4\Theta_W(s - M_Z^2)^2\sqrt{s}}, \qquad (III.70)$$

where P is the 3 - momentum of the ZA

$$P = \frac{1}{2}\left[\, s - 2M_Z^2 - 2M_H^2 + \frac{1}{s}(M_Z^2 - M_H^2)^2 \,\right]^{1/2} \qquad (III.71)$$

This cross section is plotted for various values of the Higgs mass in Fig. III.19.

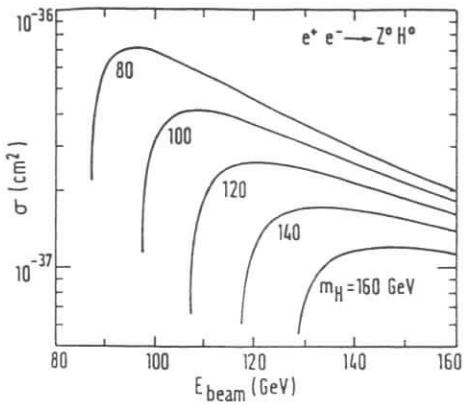

Fig. III.19: Total cross section for the process $e^+e^- \rightarrow HZ$, as a function of M_H and the beam energy.

One can see from Fig. III.19 that:

i) the cross section for $e^+e^- \rightarrow HZ$ is not too strongly energy dependent after the threshold rise.

ii) the cross section itself is smallish ($\sigma \sim 1\ pb$ for $M_H \simeq 50\ GeV$)but is measurable at LEP 200 where one hopes to be able to collect 500 pb^{-1} of data per year. For reference, remember $\sigma(e^+e^- \rightarrow W^+W^-) \sim 20\ pb$.

Of course, to actually measure this cross section one must identify the Z and so one really ends up by reducing the number of events, since not all Z decays lead to easily identifiable signals. The techniques to use are again very similar to those employed for the Higgs search at the Z pole. The cleanest signal is provided by the decays of the Z into lepton pairs, leading to processes with 2 jet back to back to an $\ell^+\ell^-$ pair. A less distinctive signal is provided by the $Z \rightarrow \nu\bar{\nu}$ decay, although this rate is six times greater than that into $\ell^+\ell^-$. The most favorable process, from the point of view of rate, would use the hadronic decays of the Z. However, the ensuing 4 jet process is difficult to separate from other 4 jet backgrounds, like W^+W^- production into 4 jets.

The feasibility of finding a Higgs boson at LEP 200 via one of the above processes has been studied in some detail by Boucrot et al [64]. These authors used a realistic detector simulation, including a track finding algorithm and pattern recognition, and made detailed background studies. In addition, they refined various analysis techniques to demonstrate what signal levels, and what Higgs masses, one could realistically expect to see at LEP 200. Their results [64] are that one can expect to dig out an 80 GeV Higgs by looking at the associated decays of the Z into either $\ell^+\ell^-$ or $\nu\bar{\nu}$. If one studies Z decays into hadrons matters are a little worse, because of confusion between the Higgs and Z generated jets. The quality of the expected signal for a 60 GeV Higgs, for the neutrino decay process of the Z is shown in Fig. III.20.

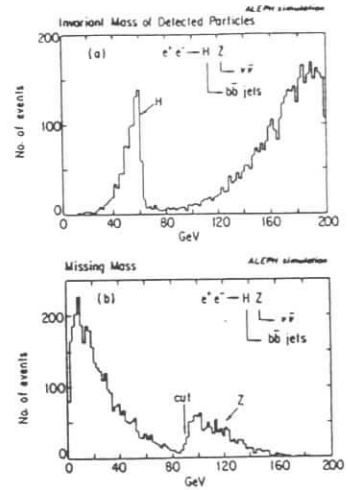

Fig. III.20: Signal for the process $e^+e^- \rightarrow HZ$, with $Z \rightarrow \nu\bar{\nu}$ and $H \rightarrow b\bar{b}$: a) Invariant mass of detected particles; b) Missing mass distribution, from [64].

If the Higgs is heavier than 80 GeV, the only hope for the detection will be through its production in hadronic colliders. However, in this case the background situation is much more severe, at least for a relatively light Higgs ($M_H \leq 2M_W$). As a full discussion of these matters would take me too long to develop properly here, I refer the interested reader to the excellent review of Cahn [60] and bring these lectures to a close.

Acknowledgements

I am grateful to D. Altschuler and J. Nieves for their excellent hospitality in Puerto Rico and for their patience in waiting for a manuscript for these lectures to materialize.

The bulk of these lectures were originally presented at the International School on Elementary Particle Physics in Duilovo, Yugoslavia, in Fall 1986 and again at the IV Swieca Winter School in Sao Paolo, Brazil, in February 1987. I am grateful to the students in these schools, as well as the students in Puerto Rico, for their useful feedback.

Some of the material in these notes is contained in my write-ups of the lectures given at the 1986 CERN School of Physics in Sandhamn, Sweden, at the 1986 XIV International Winter Meeting on Fundamental Physics in St. Feliu de Guixol, Spain, and at the 1988 TASI School in Providence, Rhode Island.

References

[1] S. L. Glashow, Nucl. Phys. 22 (1961) 579; A Salam in **Elementary Particle Theory**, ed. N. Svartholm (Almqvist and Wiksell, Stockholm, 1968); S. Weinberg, Phys. Rev. Lett. 19 (1967) 1264

[2] See, for example, E. S. Abers and B. W. Lee, Phys. Rept. 9C (1973) 1

[3] For a recent discussion, see for example, M. S. Chanowitz, Ann. Rev. Nucl. Part. Sci. 38 (1988) 323

[4] N. Cabibbo, Phys. Rev. Lett. 10 (1963) 531; M. Kobayashi and T. Maskawa, Prog. Theo. Phys. 49 (1973) 652

[5] See, for example, D. H. Perkins, Proceedings of the 1981 CERN-JINR School of Physics, Hanko, Finland

[6] F. Bergsma et al, Phys. Lett 147B (1984) 481

[7] L. A. Ahrens et al, Phys. Rev. Lett 51 (1983) 1516; 54 (1985) 18

[8] See for example, R. P. Feynman, **Photon Hadron Interactions** (W. A. Benjamin, Reading, Mass 1972)

[9] See for example, A. J. Buras, Rev. Mod. Phys. 52 (1980) 199; G. Altarelli, Phys. Rept. 81C (1982) 1

[10] C. Llewellyn Smith, Nucl. Phys. B228 (1983) 205

[11] CDHS Collaboration H. Abramowicz et al., Phys. Rev. Lett. 57 (1986) 298

[12] CHARM Collaboration J. V. Allaby et al., Phy. Lett. 177B (1986) 446

[13] CCFRR Collaboration P. G. Reutens et al, Phys. Lett. 152B (1985) 404

[14] FMM Collaboration D. Bogert et al., Phys. Rev. Lett. 55 (1985) 1969

[15] U. Amaldi et al., Phys. Rev. D36 (1987) 1385

[16] G. Costa et al., Nucl. Phys. B 297 (1988) 244

[17] CDHS Collaboration H. Abramowicz et al., Z. Phys. C 28 (1985) 51

[18] CHARM Collaboration M. Jonker et al., Phys. Lett. 99B (1981) 265: 103B (1981) 469 (E)

[19] C. Prescott et al., Phys. Lett. 84B (1979) 524

[20] A. Argento et al., Phys. Lett. 140B (1984) 142

[21] UA1 Collaboration G Armison et al., Phys. Lett. 122B (1983) 103; UA2 Collaboration M. Banner et al., Phys. Lett. 122B (1983) 476

[22] UA1 Collaboration, G. Arnison et al., Phys. Lett. 129B (1983); UA2 Collaboration P. Bagnaia et al., Phys. Lett. 129B (1983) 130

[23] P. Jenni, in Proceedings of the 1987 International Symposium on Lepton and Photon Interactions at High Energy, Hamburg, ed. W. Bartel and R. Ruckl, Nucl. Phys. B (Proc. Suppl.) 3 (1988) 341

[24] W. Marciano, Phys. Rev. D20 (1979) 274; F. Antonelli and L. Maiani, Nucl. Phys. B 186 (1981) 269; For a more extensive discussion, see also L. Maiani in TASI Lectures 1984, Univ. of Michigan, Ann Arbor, Michigan; R. D. Peccei in TASI Lectures 1988, Brown University, Providence, Rhode Island.

[25] A. Sirlin, Phys. Rev. D22 (1980) 971

[26] A. Sirlin, Phys. Rev. D29 (1984) 89

[27] W. Marciano and A. Sirlin, Phys. Rev. D12 (1980) 2695; D29 (1984) 945; M. Consoli, S. Lo Presti and L. Maiani, Nuc. Phys. B223 (1983) 474; Z. Hioki, Prog. Theor. Phys. 68 (1982) 2134; Nuc. Phys. B229 (1983) 284

[28] UA1 Collaboration C Albajar et al., Zeit. Phys. 37C (1988) 505

[29] B. Adeva et al., Phys. Rev. Lett. 55 (1985) 665

[30] P. Baillon et al., in Physics at LEP, eds. J. Ellis and R. D. Peccei, CERN Yellow Report, CERN 86-02

[31] M. L. Swartz in Polarization at LEP, eds. G. Alexander et al., CERN Yellow Report, CERN 88-06

[32] See for example, Polarization at LEP eds. G. Alexander et al., CERN Yellow Report, CERN 88-06

[33] B. W. Lynn and R. G. Stuart, Nucl. Phys. B 253 (1985) 216; B. W. Lynn and C. Verzegnassi, Phys. Rev. D 35 (1987) 3326; B. A. Kniehl, J. H. Kuhn and R. G. Stuart in Polarization at LEP, eds. G. Alexander et al., CERN Yellow Report, CERN 88-06

[34] D. Treille in Polarization at LEP, eds. G. Alexander et al., CERN Yellow Report, CERN 88-06

[35] J. Chaveau in Physics at LEP, eds. J. Ellis and R. D. Peccei, CERN Yellow Report, CERN 86-02

[36] M. Consoli and A. Sirlin in Physics at LEP, eds. J. Ellis and R. D. Peccei, CERN Yellow Report, CERN 86-02

[37] T. Appelquist and H. Georgi, Phys. Rev. D8 (1973) 4000; A. Zee, Phys. Rev. D8 (1973) 4038

[38] See, for example, the recent global analysis by A. Ali and F. Barreiro, DESY preprint DESY 88-075

[39] R. Kleiss in Physics at LEP, eds. T. Ellis and R. D. Peccei, CERN Yellow Report, CERN 86-02

[40] G. Altarelli in Physics at LEP, eds. J. Ellis and R. D. Peccei, CERN Yellow Report, CERN 86-02

[41] A. Blondel et al., in **Physics at LEP**, eds. J. Ellis and R. D. Peccei, CERN Yellow Report, CERN 86-02

[42] For a recent review, see for example, R. D. Peccei in Proceedings of the Flavor Symposium, Beijing, August 1988

[43] E. Ma and J. Okada, Phys. Rev. Lett. 41 (1978) 287; K.J.F. Gaemers, R. Gastmans and F. M. Renard, Phys. Rev D19 (1979) 1605; G. Barbiellini, B. Richter and J. L. Siegrist, Phys. Lett. 106B (1981) 414

[44] E. Simopoulou in **Physics at LEP**, eds. J. Ellis and R. D. Peccei, CERN Yellow Report, CERN 86-02

[45] M. Caffo, R. Gatto and E. Remiddi, Phys. Lett 173B (1986) 91; Nucl. Phys. B 286 (1987) 293

[46] C.Maña and M. Martinez, Nucl. Phys. B 287 (1987) 601; See also, F.A. Berends et al., Nucl. Phys. B 301 (1988) 583

[47] J. Bartels, A. Fridman, T. T. Wu and A. Schwarz; Z. Phys. C23 (1984) 295

[48] O. P. Sushkov, V. V. Flambaum and I. B. Khriplovich, Sov. J. Nucl. Phys. 20 (1975) 537

[49] W. Alles, Ch. Boyer and A. J. Buras, Nucl, Phys. B119 (1977) 125

[50] J. M. Cornwall, D. M. Levin and G. Tiktopoulos, Phys. Rev. Lett. 30 (1973) 1268, (E) 31 (1973) 572; Phys. Rev. D10 (1974) 1145; (E)D 11 (1975) 972; C. H. Llewellyn Smith, Phys. Lett. 46B (1973) 233; S. D. Joglekar, Ann. Phys. (NY) 83 (1974) 427

[51] G. Barbiellini et al., in **Physics at LEP**, eds. J. Ellis and R. D. Peccei, CERN Yellow Report, CERN 86-02

[52] T. D. Lee and C. N. Yang, Phys. Rev. 128 (1962) 885

[53] K. Hagiwara, R. D. Peccei, D. Zeppenfeld and K. Hikasa, Nucl. Phys. B282 (1987) 253

[54] K. J. Gaemers and G. J. Gounaris, Z. Phys. C1 (1979) 259

[55] See, for example, the Proceedings of the ECFA Workshop on LEP 200, eds. A. Bohm and W. Hoogland, CERN 87-08

[56] P. Roudeau et al. in Proceedings of the ECFA Workshop on LEP 200. eds. A. Bohm and W. Hoogland, CERN 87-08

[57] M. Luescher and P. Weisz, Nucl. Phys. B290 [FS 20] (1987) 25; B295 [FS 21] (1988) 65; Phys. Lett. 212B (1988) 472

[58] J. Kuti, L. Lin and Y. Shen, Phys. Rev. Lett. 61 (1988) 678

[59] B. W. Lee, C. Quigg, and H. B. Thacker, Phys. Rev. D16 (1977) 1519

[60] R. N. Cahn, LBL-25092, to be published in Reports on Progress in Physics (1988). See also [3]

[61] J. D. Bjorken, Proceedings of the 1976 SLAC Summer Institute on Particle Physics, ed. M.C. Zipf (SLAC-198, 1977)

[62] H. Baer et al., in **Physics at LEP**, eds., J. Ellis and R. D. Peccei, CERN Yellow Report, CERN 86-02

[63] B. L. Ioffe and V. A Khoze, Sov. J. Part. Nucl. 9 (1978) 50; B. W. Lee, C. Quigg and H. B. Thacker, Phys. Rev. D16 (1977) 1519; R.L. Kelly and T. Shimada, Phys. Rev. D23 (1981) 1940

[64] J. Boucrot et al., in Proceedings of the ECFA Workshop on LEP 200, eds. A. Bohm and W. Hoogland, CERN 87-08.